



## CHAPTER IV

### RESULTS AND DISCUSSIONS

#### 4.1 Characterization of Blank Samples

The characterizations of blank samples were carried out in order to establish baseline information of surface morphology and chemistry as well as its chemical depth profile which were used as comparative references against the treatment samples including those of Hg adsorptions and Hg decontamination experiments, respectively. The details of the characterization are presented as follows:

##### 4.1.1 Manufacturer Specifications

The blank samples, steel coupons employed in the study, were cut from new subsea pipeline with specifications of the American Petroleum Institute (API); 5L-X52 for line pipe specifically uses for oil and gas transportation. The chemical compositions of API 5L-X52 is presented in Table 1-1 below:

**Table 4-1** Chemical Compositions of API 5L-X52 Pipeline

Chemical Composition (weight %)		
C 0.18	Cr 0.07	Nb <0.001
S <0.01	Ni 0.12	Ti 0.019
Mn 0.94	Mo 0.03	W <0.006
P 0.009	Cu 0.206	Fe Balance
Si 0.23	V 0.003	

Source; Rodriguez 2007

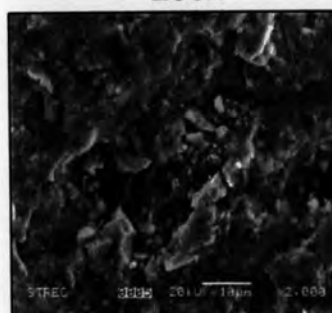
Table 4-1 shows that Fe is the dominant component of the material. Moreover, other minor elemental constituents are Cr, Mn, Ni, Si, etc. which make the material to become alloy contributing to objective of the material utilization as petroleum pipeline.

#### 4.1.2 Surface Morphology

Characterization of surface morphology of the blank coupons was undertaken using Scanning Electron Microscope (SEM). The surface morphology of the blank sample, under various SEM magnifications, is illustrated in Figure 4-1 below:



200x



2000x



5000x

**Figure 4-1** Surface morphology of a blank sample

Figure 4-1 shows that the surface morphology of the blank coupon is irregular and heterogeneous. The closer examination under higher resolutions found surface pits and crevices which act as potential adsorption sites for elemental Hg.

#### 4.1.3 Surface Chemistry

Characterization of the blank surface chemistry was undertaken using the SEM-EDS. The examinations were undertaken with each batch of material employed of which the results are presented as the following:

**Table 4-2** Average surface chemical compositions of the blank samples analyzed by the EDS technique

Elements	%Element	%Atom
C	11.39±4.21	29.86±5.84
O	12.55±6.40	24.18±9.13
Mn	0.85±0.13	0.51±0.16
Fe	75.22±10.44	45.45±14.42
Total	100	100

Table 4-2 shows that Fe is dominant elemental component of the blank coupon surface in terms of both % atom and % element by the EDS analysis. It also contains considerable levels of C and some Mn which are consistent with its provided specifications. Oxygen (O) detected on the blank surface, may indicate the surface oxide layer. The results surface chemistry served as baseline information of the steel coupon before they were employed in the following experiments;

#### 4.1.4 Chemical Depth Profile

The characterization of chemical depth profile of the blank coupon was carried out using the X-ray Photoelectron Spectroscopy (XPS) technique. A numbers of steps of etching were undertaken to a total depth of approximately 350 nanometer (nm). The results of the chemical depth profile of the blank coupon are presented in Figure 4.2 below:

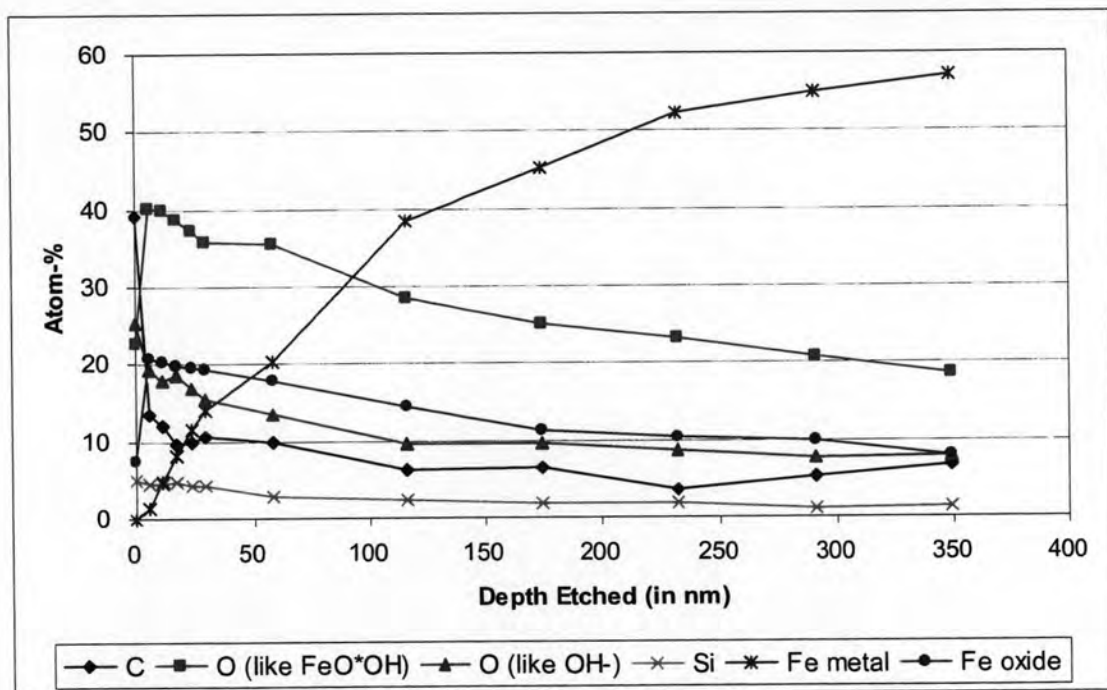


**Figure 4-2** Chemical depth profile of a blank sample

Figure 4-2 shows the following:

- Fe-metal gradually increases from the surface through the course of the depth profile analyzed prior to becoming more predominant and persistent at the depth of about 350 nm;
- O (like OH-) gradually declines from the surface and becomes persistent at the depth of approximately 120 nm. The OH-like O detected may be an intermediate in Fe corrosion process;

- Si slowly declines and become persistent at the depth after 50 nm approximately;
- C decreases rapidly to the depth of approximately 30 nm prior to being more persistent at the depth after 100 nm which continues throughout the depth profile analyzed;
- Similar patterns of depth profile between Fe-oxide and O (like FeO\*OH) are observed to increase rapidly at the top surface (about 5-10 nm) before they gradually decrease throughout the course of the depth profile. Both of Fe-oxide and FeO\*OH are considered to be products of iron corrosion indicating that the top surface of the blank coupons was oxidized; and
- The depth profile of O (like FeO\*OH) found in the experiment is very similar to that reported by Zalavutdinov (2001). He also found that O on the surface of F82H steel analyzed using Ion Mass Spectrometry (SIM) analysis showed rapid increase at the topmost surface prior to its gradual decrease through the course of the depth profile until to a total depth about 450 nm.

#### **4.2 Mercury Adsorption**

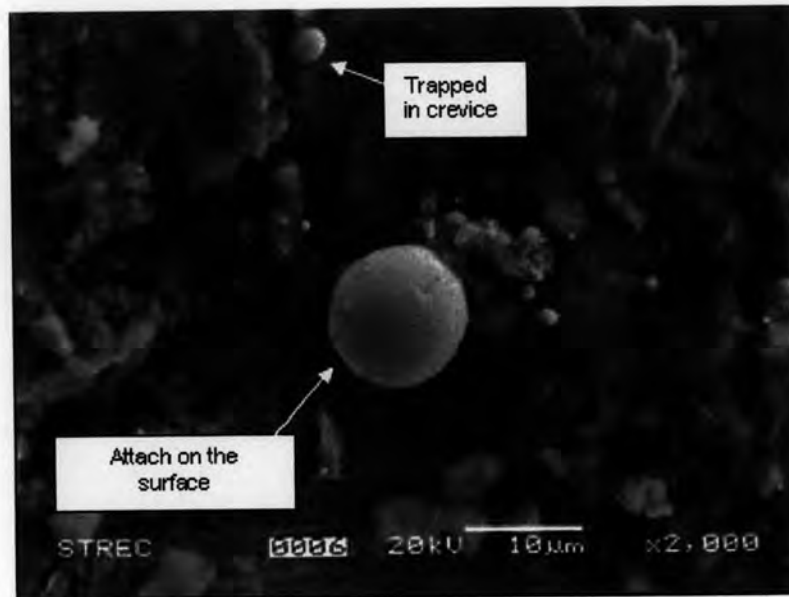
Mercury adsorption was undertaken by immersing the uncoated internal surface of the steel coupons into liquid elemental mercury at the controlled temperature of 25 °C. The adsorptions were continued for 15, 30, 45, 60, 75 and 90 days, respectively, before they were retrieved and then submitted for surface laboratory analyses. The analyses were designed and carried out in order to characterize different species of mercury at different time intervals taking into account availability of analytical instruments in the country, time required for shipment, etc. The details of the analysis are detailed below:

- SEM-EDS analysis; was undertaken within 24 hours after upon reaching the pre-determined Hg adsorption periods. SEM was used to characterize surface morphology of the Hg adsorption coupons, whereas EDS was used to quantitatively analyze total surface Hg levels in all Hg forms including elemental Hg, but without identification of Hg speciation;
- XRD analysis; was undertaken no later than a week after the samples were submitted to laboratory for the analyses. The XRD analysis was used to analyze crystalline compounds that may present on the coupon surface. The XRD technique may not possibly be used to detect elemental Hg due to its non-crystalline structure; and
- XPS analysis; was undertaken no later than 2 weeks after the samples had reached their pre-determined adsorption periods due to the time required for shipment of the samples to Chevron Research Center, located in Richmond, California. The XPS technique could analyze all speciation of Hg that might present on the surface and in the depth profile due its high spectra resolution.

The discussions of the results of the adsorption experiments will take into account these analytical sequences of analysis in order to provide consistent basis for data analysis, interpretation and discussion, respectively.

#### **4.2.1 Surface Morphology – Hg Adsorption**

The illustrations of Hg on the surface of steel coupon at different adsorption days are presented in Figure 4-3 below:



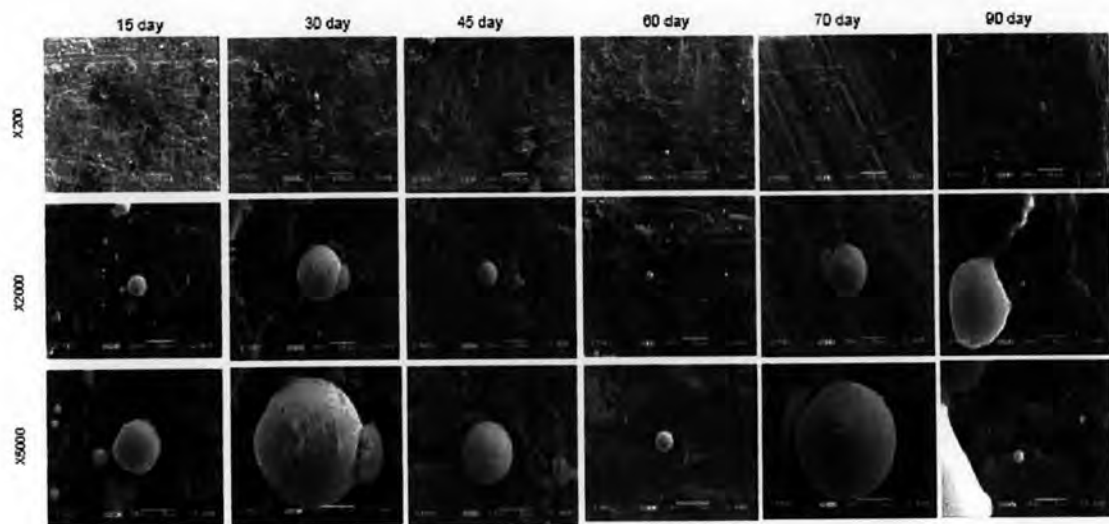
**Figure 4-3** Hg adsorption on the steel coupon surface

Figure 4-3 shows the following:

- Various sizes of spherical-shaped mercury droplets were observed on the steel coupon surface. The bigger droplets could be greater than 10  $\mu\text{m}$ , whereas the smaller sizes could be less than 1  $\mu\text{m}$ ;
- Distribution of Hg droplets on the surface was not consistent and heterogeneous in respecting to both surface adsorption locations and also the droplet sizes. However, the bigger droplets tended to attach on the steel coupon surface, whereas the smaller tended to fall into the pits or crevices present on the surface which could be seen as darker spots on Figure 4-3;
- These findings are consistent with a study undertaken by Zettlizer in 1997 that he analyzed steel samples collected from equipment, well tubing and pipeline used in a natural gas field in North Germany with presence of mercury in the petroleum crudes and found that mercury deposition occur on the surface

in different manners including; a) at previously damaged sites of the steel component, such as corrosion pits or open stress cracks and b) in the pores in the steel, which communicate with the surface by way of channels (Zettlitzer, 1997).

The surface morphology of Hg adsorption of 15, 30, 45, 60 and 90 days respectively, is illustrated in Figure 4-5 below:



**Figure 4-4** SEM illustration of Hg adsorption on the coupon surface of 15, 30, 45, 60, 75 and 90 day Hg adsorption

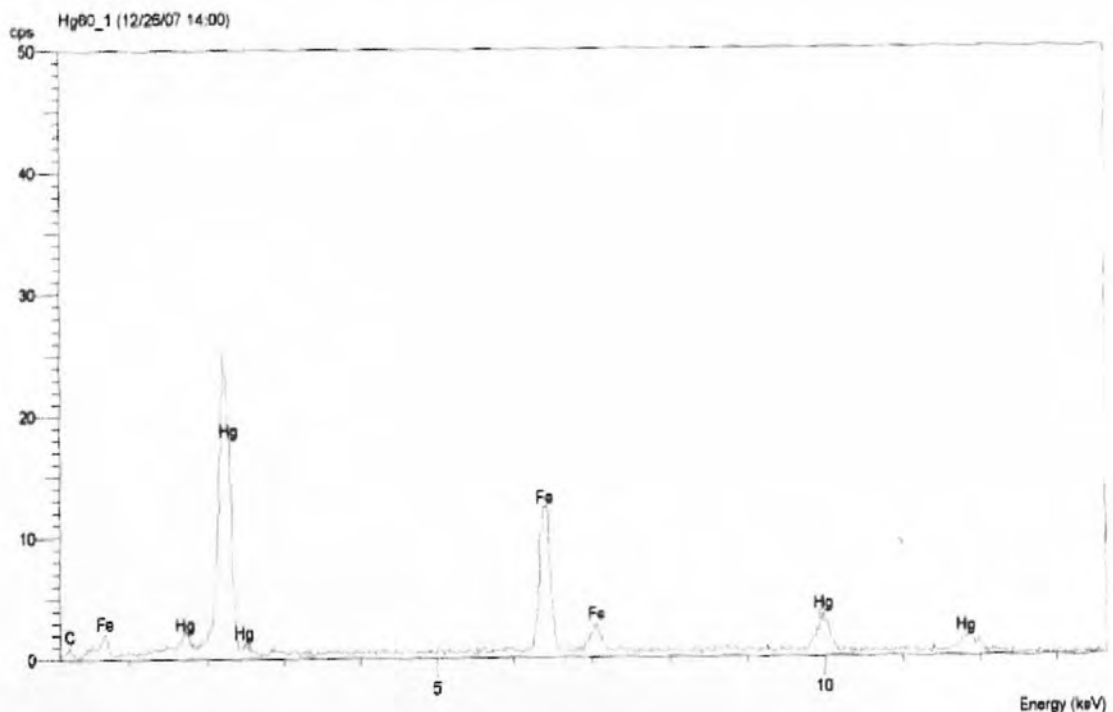
Figure 4-4 shows irregularities in distribution of Hg droplets on the surface of Hg adsorption coupons. The adsorption of Hg, as discussed earlier, is not in the function of the adsorption periods only, but also surface characteristic which favors Hg adsorption. Due to heterogeneity of mercury distribution, different areas on the surface were therefore had to be analyzed using the different surface analysis techniques discussed.



## 4.2.2 Surface Chemistry – Hg Adsorption

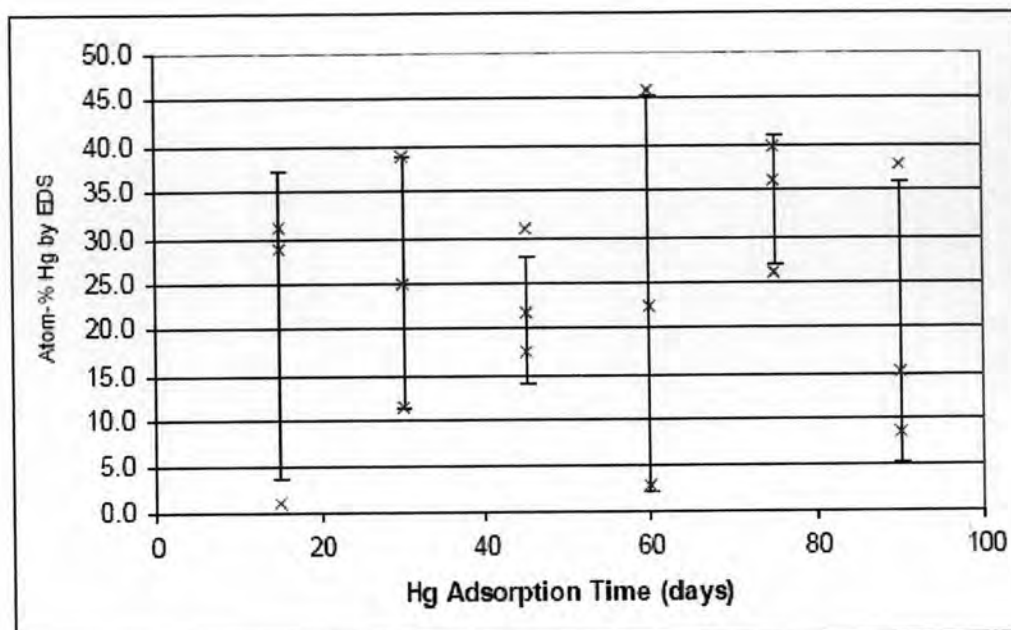
### 4.2.2.1 EDS Analysis – Hg Adsorption

The surface Hg levels of the Hg adsorbed coupons were analyzed using SEM-EDS technique. The analysis was undertaken shortly after reaching each predetermined adsorption period at three different locations across the coupon surface all of which the results are presented in Figure 4-5 and Figure 4-6 below:



**Figure 4-5** EDS profile of a 60 day Hg adsorption steel coupon sample

The results of EDS analysis of blank and Hg adsorption coupons are presented in Appendix A. It is noted that the standard error and detection limit of the analysis are 10% and 1 % atom of Hg respectively.



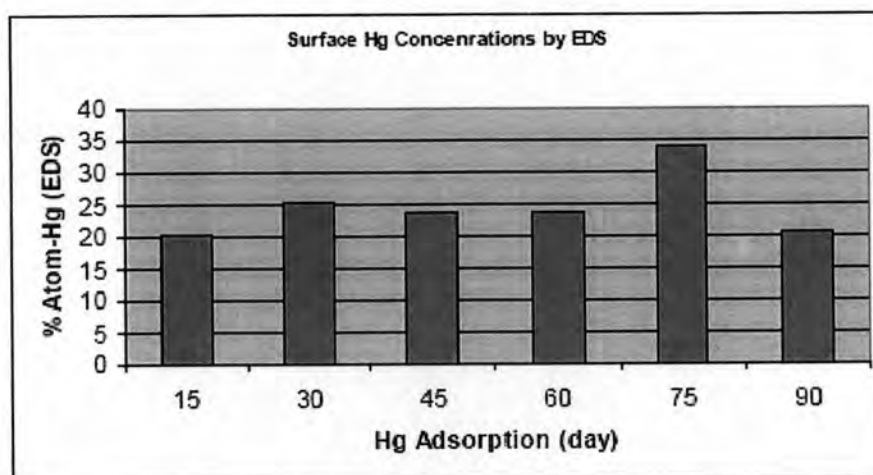
**Figure 4-6** EDS results of Hg on the surface of the adsorption samples

Figure 4-6 shows the following:

- There is no reasonable correlation existed between Hg adsorption periods and average Hg concentrations as can be seen from high fluctuation of surface Hg levels on each Hg adsorption treatment. As discussed earlier that another confounding factor, beside Hg adsorption periods, is the heterogeneous surface characteristic that may contribute to high variation of surface Hg concentrations;
- Statistical analysis of the EDS surface Hg results using Single-factor ANOVA technique found the  $F_{critical}$  value of 3.10 which is greater than the  $F_{(0.05,5,12)}$  value of 0.35 at 95% degree of confident. This indicates that they are not significantly different between average surface Hg concentrations in each of these Hg adsorption periods.
- EDS analysis was undertaken in conjunction with SEM observations under which droplets of elemental Hg were

observed. However, It is hard to conclude at this stage that right after Hg adsorption there was the only elemental Hg present on the coupon surface beside other possible speciation such as HgO without confirmation of the results using other specific surface analytical techniques e.g. XPS.

Based on the EDS surface Hg measurements, the average % atom-Hg of each Hg treatment can be presented in Figure 4-8 below:



**Figure 4-7** Average % atom-Hg on the surface of Hg adsorption samples

Figure 4-7 shows that the highest average surface Hg concentrations were observed at 75<sup>th</sup> day of approximately 35 % atom-Hg by EDS. At 30<sup>th</sup>, 45<sup>th</sup> and 60<sup>th</sup> day Hg adsorption respectively, surface Hg concentrations are in proximity to 25 % atom-Hg by EDS. The lowest concentrations were found on 15 and 90 day treatments when the surface Hg concentrations are approximately 20 % atom-Hg by EDS.

Based on the results of the surface Hg levels above, the groups of Hg adsorbed coupons could be categorized into the following:

- Group 1: low initial Hg levels; 15 and 90 day Hg treatments;
- Group 2: moderate initial Hg levels; 30, 45 and 60 day Hg treatments; and
- Group 3: high initial Hg levels; 75 day Hg treatment.

The categorization was subsequently used in selection of set of Hg treatments used in the depth profile analysis for Hg decontamination experiments.

#### 4.2.2.2 XRD Analysis – Hg Adsorption

As mentioned earlier, the XRD analysis was undertaken no later than a week after SEM-EDS analysis. The analysis was undertaken to characterize crystalline chemical compounds present on the surface of Hg adsorption samples. The results of XRD analysis are presented in Appendix B with the overall XRD profile shown in Figure 4-8 below:

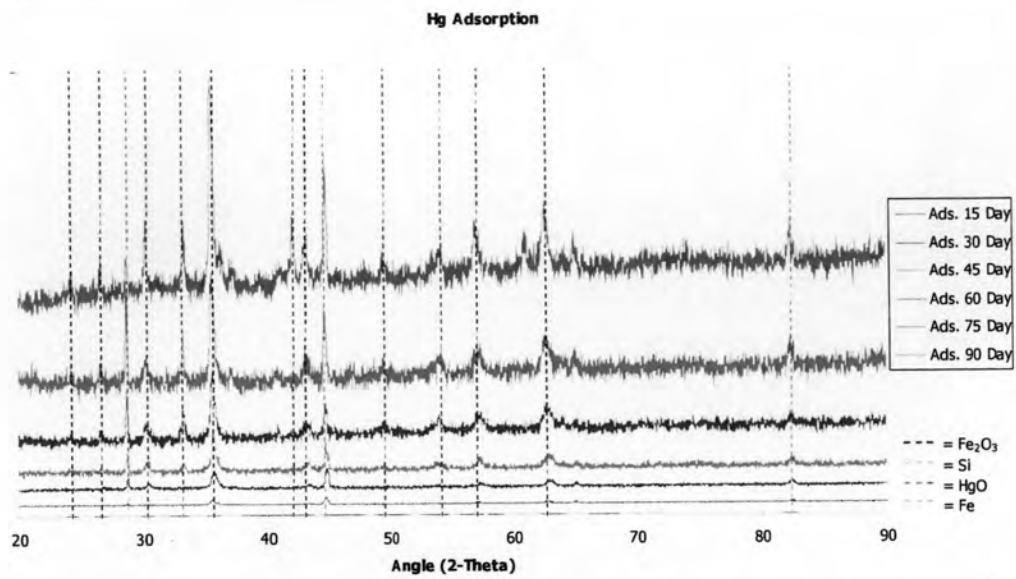
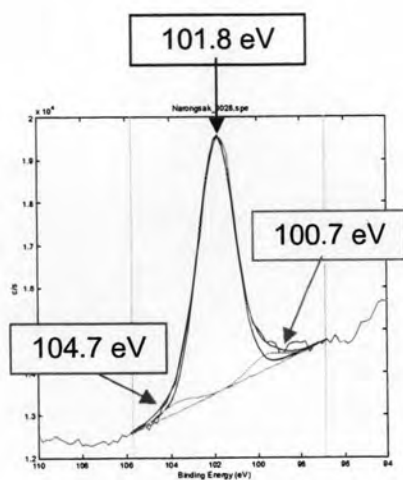


**Figure 4-8** XRD profile of 15 - 60 day Hg adsorption sample

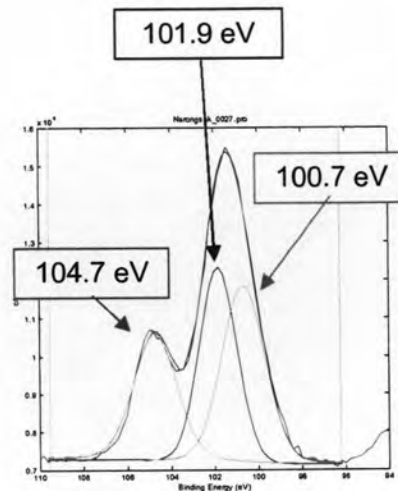
Figure 4-8 shows the presence of crystalline substances that were detected on the Hg adsorbed coupon surface the surface including Fe-metal, Fe<sub>2</sub>O<sub>3</sub>, Si and HgO on all Hg treatment coupons of 15 – 90 day. The results show that other Hg form of HgO was detected after no later than a week of the analysis.

#### 4.2.2.3 XPS – Hg Adsorption

The XPS analysis were undertaken at four different locations across the Hg adsorbed coupon surface of which the results and discussions are presented as the following:



**Hg30**, topmost surface



**Hg90**, topmost surface

**Figure 4-9** XPS Profile of Hg species on the topmost surface of Hg adsorption samples

The results of XPS analysis show that XPS spectra of Hg4f7/2 were observed with binding energy of 100.7 eV. Matching of the detected to the published binding energies revealed that it matched to those of the oxide state of Hg4f7/2 (100.5-101.0 eV). This shows that with the XPS analysis after no later than two weeks, HgO is the only speciation that found on the surface of Hg adsorbed coupons. The published binding energies are presented in Table 4-3 below:

**Table 4-3** Published binding energies of Hg

Elements	Binding energy of metallic state(eV)	Binding energy of oxide state (eV)
Hg4f7/2	99.5-100.0	100.5-101.0

Source; Motohiro 2003

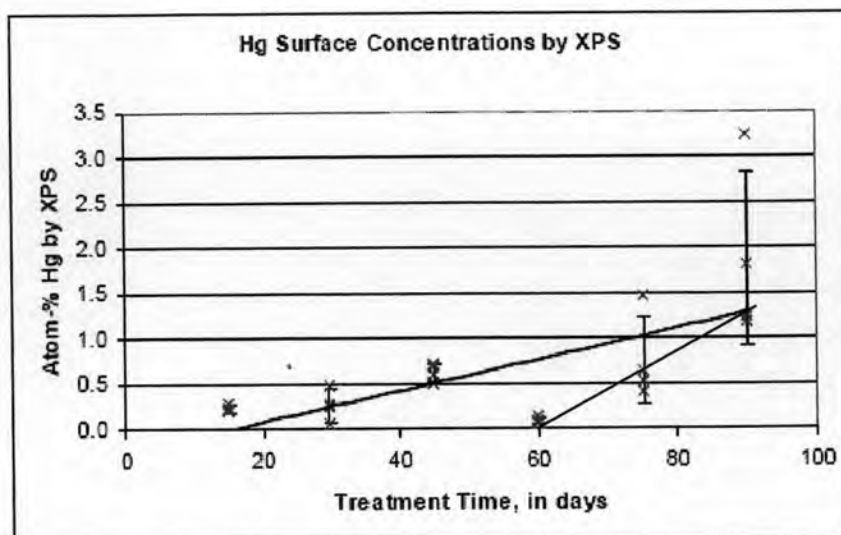


**Figure 4-10** Hg levels on adsorption samples by XPS method

Figure 4-10 shows that there is no reasonable correlation existed between Hg adsorption periods and %atom of Hg by the XPS on the Hg adsorbed surface coupons. The statistical analysis using Single-factor ANOVA technique revealed the  $F_{critical}$  value of 2.77, which is below the  $F_{(0.05,5,18)}$  value of 8.52. This indicates that average surface Hg levels by the XPS are significantly different in each of Hg adsorption periods at 95 % degree of confident.

Two possible increasing trends of surface Hg were observed at 15 and 60 days, respectively. This may be due to peel-off phenomena of HgO deposit on the metal surface over certain periods of time. At 60<sup>th</sup> day, HgO deposit may peel off resulting in restarting of new increasing Hg trend on the top surface at 60<sup>th</sup> day. The HgO peel-off phenomena on metal surface adsorbed with Hg was also reported by Zalavutdinov in 2001.

It is therefore questionable of how Hg on the topmost surface of the Hg adsorbed coupons was oxidized to HgO and where the Oxygen (O) in the molecule of HgO possibly come from; either from the air upon direct exposure of metal coupon to the atmosphere after completion of Hg adsorption or from other metal oxide compounds e.g.  $Fe_2O_3$  that initially

present on the surface and was detected in the blank coupon prior to Hg adsorption.

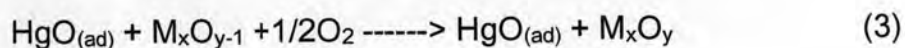
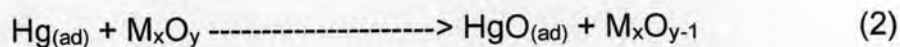
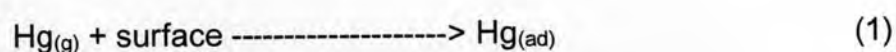
Reviewing the relevant literature found that HgO can be synthesized by heating of Hg up to 350 °C in the air (Greenwood, 1997). Withstanding this, formation of HgO on the metal coupon surface through Hg oxidation with oxygen in the air is thermodynamically unfavorable.

Other potential HgO forming reaction and mechanism were therefore investigated and found that many metal oxides have been used to capture Hg such as CuO, Cu<sub>2</sub>O, MnO<sub>2</sub>, V<sub>2</sub>O<sub>5</sub>, Cr<sub>2</sub>O<sub>3</sub>, TiO<sub>2</sub>, Fe<sub>2</sub>O<sub>3</sub>, etc. It is suggested that lattice oxygen of metal oxide could also serve as the oxidant of Hg (Zhijian, 2008).

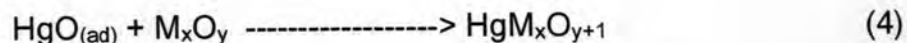
It is also indicated by using Gibbs formation energy of Hg to HgO that Hg is seldom oxidized by O to become HgO with Gibbs formation energy of -59 kJ/mole (Motohiro, 2003).

The reactions involve oxidation of lattice oxygen was further elaborated that adsorbed elemental Hg reacts with lattice oxidant following heterogeneous reaction mechanism known as Mars-Maessen Mechanism (Granite, 2006).

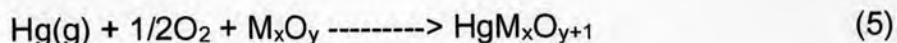
The reaction mechanism for the capture of Hg by oxide catalyst can be shown below: (Granite, 2000)







The overall reaction in the presence of gas phase oxygen is the sum of reactions steps one through four:



However, it is noted here that based on the results of the XPS analysis of the Hg adsorbed steel coupons, the final products of complex Hg and metal oxide as shown in (5) was not observed. There were only HgO and Fe<sub>2</sub>O<sub>3</sub> detected by the XPS analysis on the surface of Hg adsorbed coupons.

It was also reported that Fe<sub>2</sub>O<sub>3</sub> could possible enhance elemental Hg oxidation on fly ash particles with more specific details as the following: (Granite, 2006)

- Fe<sub>2</sub>O<sub>3</sub> in model fly ash (fixed bed) catalyzed Hg oxidation;
- α -Fe<sub>2</sub>O<sub>3</sub> injected into flue gas had little catalytic ability;  
and
- γ -Fe<sub>2</sub>O<sub>3</sub> coated onto fabric filters enhanced Hg oxidation.

It was reported on another study that based on bench-scale investigations, NO, NO<sub>2</sub>, α -Fe<sub>2</sub>O<sub>3</sub> and γ -Fe<sub>2</sub>O<sub>3</sub> and HCl promote the conversion of gaseous elemental mercury to gaseous oxidized mercury and/or associated mercury in simulated coal combustion flue gases (Galbreath, 2004).

Finally, a study conducted on martensitic and austenitic steels after exposure in mercury at 573 K up to 5000 hour showed that the preferable places for HgO nucleation were the oxidized steel surfaces. The XRD data showed that oxides formed on the steels investigated had different structures, depending on steel chemical composition. It is likely that on F82H

steel covered with Fe<sub>2</sub>O<sub>3</sub> the HgO nucleation occurs easier than on 316L and MANET-II steels that were covered with Fe<sub>3</sub>O<sub>4</sub> and mixture of Fe<sub>3</sub>O<sub>4</sub> and Fe<sub>2</sub>O<sub>3</sub>, respectively (Zalvutdinov, 2001).

All the above results confirm the feasibility of Hg oxidation through Fe<sub>2</sub>O<sub>3</sub> mechanism which can be written in chemical reaction below:



However, benchmarking of surface Hg levels between those reported by EDS (done soon after Hg adsorption) and XPS (done no later than two weeks after Hg adsorption) shows significant reduction of concentrations of surface Hg from elemental Hg to HgO form, respectively as shown in Figure 4-11 below:

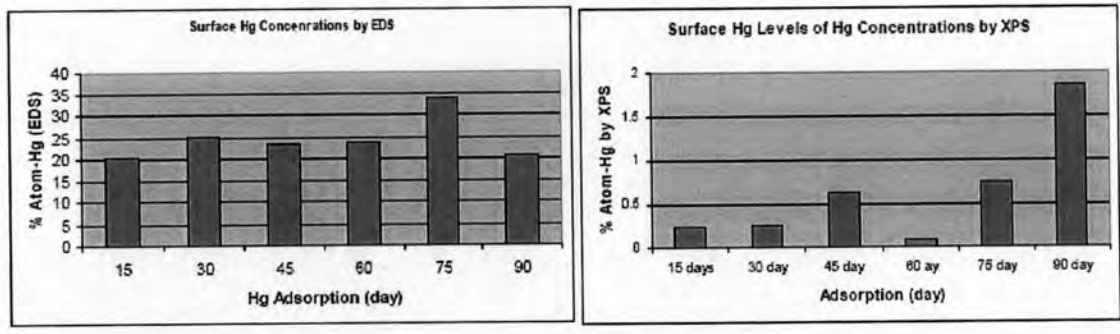


**Figure 4-11** Relative benchmarking of average % Atom-Hg on the surface of Hg adsorption samples by EDS (measured soon after reaching pre-determined contamination periods) and XPS (measured two weeks later)

The benchmarking of measurement between EDS and XPS takes into account the different sampling depth of both techniques. XPS is a surface-sensitive method whose sampling depth is limited by the finite mean free path of the photoelectrons. In contrast, EDS measures at the greater area and depth. It shows that if target elements are more consolidated on the surface, XPS techniques will report 2-5 higher target element concentrations (Morris, 2002).

It implies that if EDS were to be used to analyze surface Hg no later than 2 weeks, it may not be able to detect such low concentrations of Hg present on the surface as it could be detected by the XPS as shown in Figure 4-11. Figure 4-11 suggests that the concentrations of surface Hg by XPS were predominantly below 1.0 % atom of Hg and those could not be possibly detected by the EDS technique with the detection limit of > 1.0% atom of Hg.

However, Figure 4-11 shows that the surface Hg levels between EDS and XPS analysis are about 20-35 time differences which may not be possibly due to only the different of the analysis techniques but also the time of the analysis. This shows that at different analysis time, not only forms of Hg were found differently but also their surface concentrations. The measurements of Hg vapor in headspace of Hg adsorption coupon containers using Jerome meter in the laboratory before each analysis found that there were high Hg vapor detected. It shows that losses of Hg from the surface may be contributed by Hg volatilization process.

The results also suggest that Hg contaminated steel can potentially give off Hg vapors during their transportation and handling and thus control and mitigation measures have to be in place. For instances, they should be put in tightly sealed container, monitoring of Hg vapor to be carried out, etc. In-situ Hg decontamination may be a better approach later than retrieving and handling the Hg contaminated materials onshore in terms of both control the losses of Hg vapor and also prevention of Hg contamination into the environment. After decommissioning of subsea pipeline, it can be emptied and air can be supplied inside to facilitate Hg volatilization. The generated exhaust can be directed into a filter unit containing metal oxide catalyst that commonly used in gas treatment process, to remove Hg from the exhaust air prior to discharge into the atmosphere.

The XPS results also suggest that Hg left on the steel coupon surface after volatilization are in HgO specie, that form surface deposit similar

to iron rust. The deposit will gradually peel off from the steel surface and can potentially distribute and contaminate the surrounding environment. This is ascertained by the results of a study on martensitic and austenitic steels after exposure to liquid mercury at 573 K up to 5000 hours which found that a layer of mercury oxide was formed and peeled off (Zalavutdinov, 2001). Withstanding this, HgO deposit on the internal surface of petroleum pipeline is yet to be removed, but with much lower concentrations that make it more feasible employing in-situ decontamination technique.

#### **4.4.2 Depth Profiling – Hg Adsorption**

The depth profile analysis of the Hg treatment samples had been undertaken by using XPS techniques no later than two weeks after Hg adsorption. The results of the analysis are discussed below:

##### **4.2.2.1 Forms of Hg on the Surface and in the Depth Profile**

The experiment was conducted to characterize the Hg forms, present on the topmost surface and in the depth profile by using the XPS technique. The results of the analysis are presented in Figure 4-14 below:

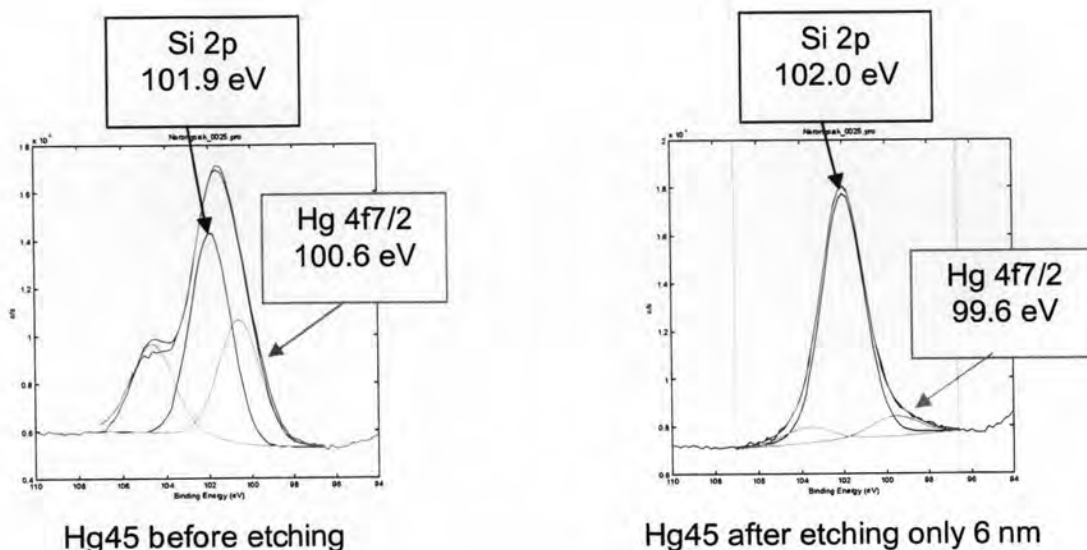


**Figure 4-12** Depth profile of Hg at the surface and after etching only 6 nm of Hg 45 day adsorption sample

Figure 4-12 shows that Hg found on the surface of Hg adsorbed coupons is in oxidized state of Hg(II) with the binding energy of 100.6 eV of Hg4f7/2 as discussed earlier. However, after a brief etching for only 6 nm from the topmost surface, Hg was found in zero valence state of elemental form with the binding energy of 99.6 eV for Hg4f7/2 as compared to the published binding energies of elemental Hg presented in Table 4-3.

It was therefore questionable if HgO was prone to ion-gun induced reduction which converted it to Hg during the etching process. As a result, an etching experiment was therefore undertaken with HgO of which the results are presented as the following:

The commercially available HgO was obtained (Acros Orgic, mercury(II)oxide yellow with 99+%) for the experiments, the results of surface scanning and depth profiling are presented as the following:

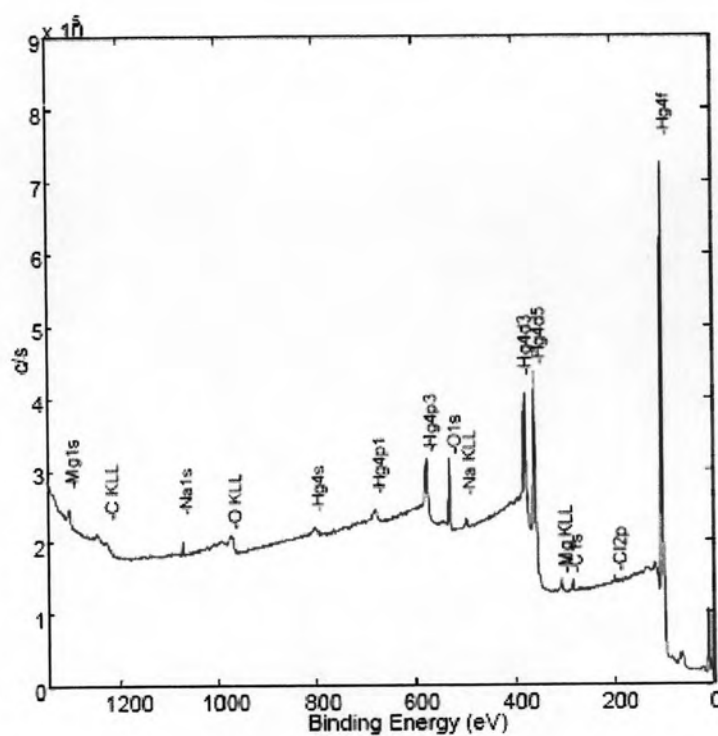


**Figure 4-13** XPS profiles of HgO

Figure 4-13 shows that HgO has only small concentrations of impurities observable. Of these, C is present at the largest concentration, which is about 20 % atom, to be consistent with expected adventitious carbon.

The etching of HgO was undertaken to the depth of about 700 nm of which the results of the depth profile analysis by is presented in Figure 4-14 below:

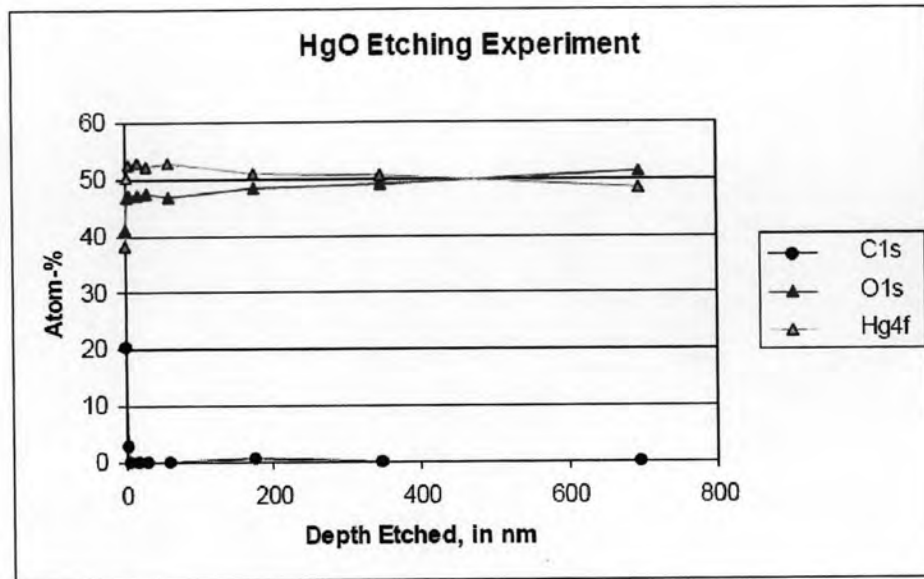


**Figure 4-14** Depth profile of HgO showing C, O and Hg

Based on the Figure above, there is no evidence to suggest decreasing of O content with etching of HgO. Only the superficial adventitious C concentration decreases substantially with depth. The calculation of Hg/O atomic ratio was therefore undertaken throughout the course of the depth profile of which the result is presented in Figure 4-15 below:

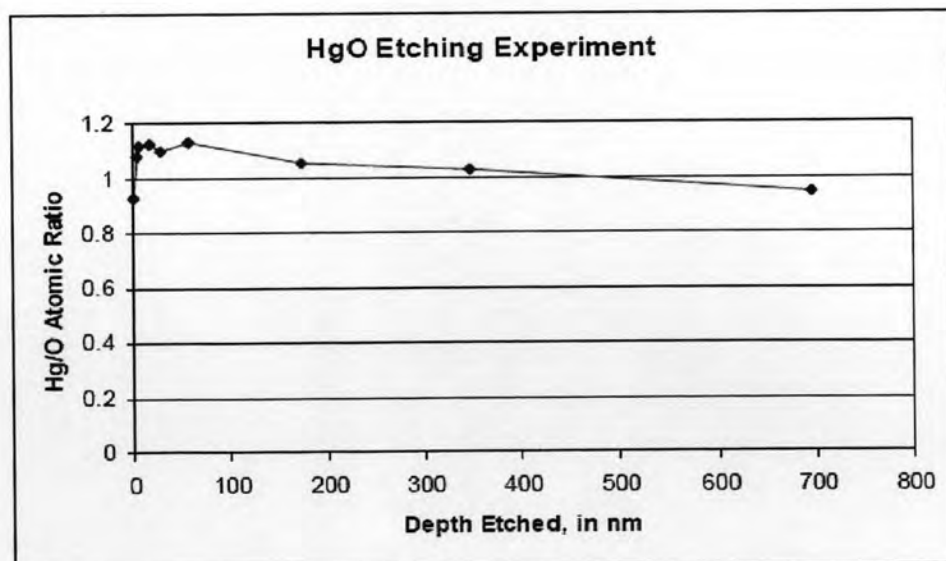


**Figure 4-15** Atomic Ratio of Hg/O throughout the Depth Etched

Based on the figure above, it shows that the ratio of Hg/O remains close to 1.0 throughout the depth. Withstanding these finding the conclusion could be drawn as the following:

- There is no evidence of ion-gun induced reduction observed for HgO;
- The change in Hg oxidation state observed for the coupons during the depth profiling experiment is not due to instability of HgO to the ion beam bombardment; and
- The observation of HgO at the surface and metallic Hg at the smallest depths is not an experimental anomaly, but a reliable experimental observation.

#### 4.2.2.2 Depth Profile Hg Reduction and Fe Oxidation

The surface of the Hg adsorption steel coupons was etched for 12 different steps such that profile of chemical composition from the top surface up to a total depth of about 350 nm was analyzed. During the XPS depth profile analysis, it was found that in different Hg treatments, different thicknesses of iron-oxide layers were observed in the XPS spectra of which the results are presented in Figure 4-16 to 4-18 below:



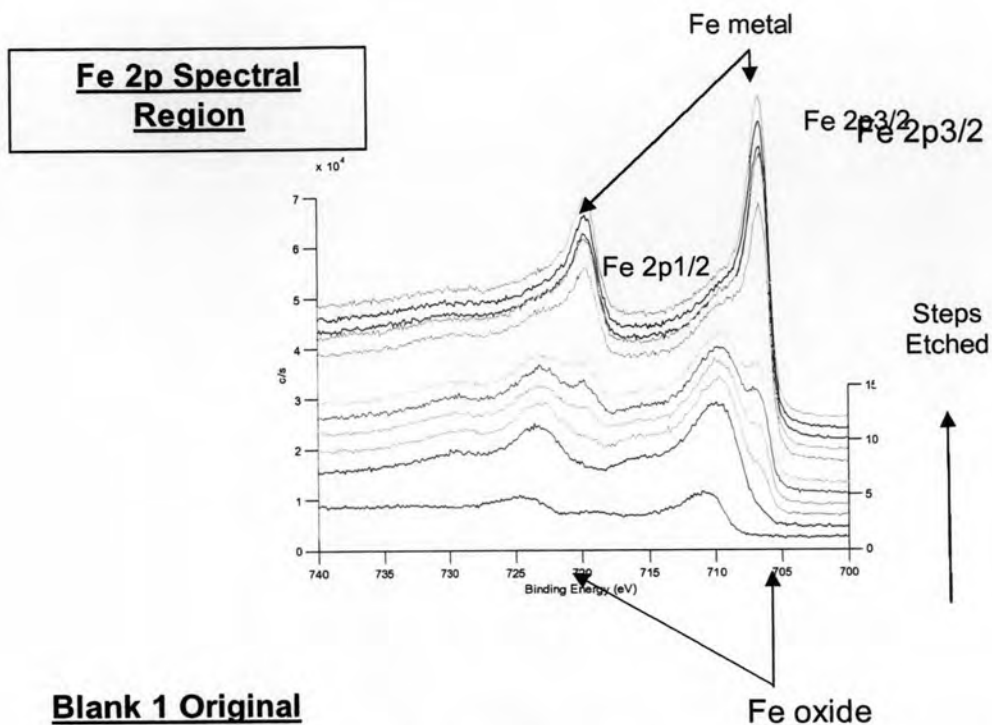


Figure 4-16 Depth profile by XPS – Oxide layers on a blank sample

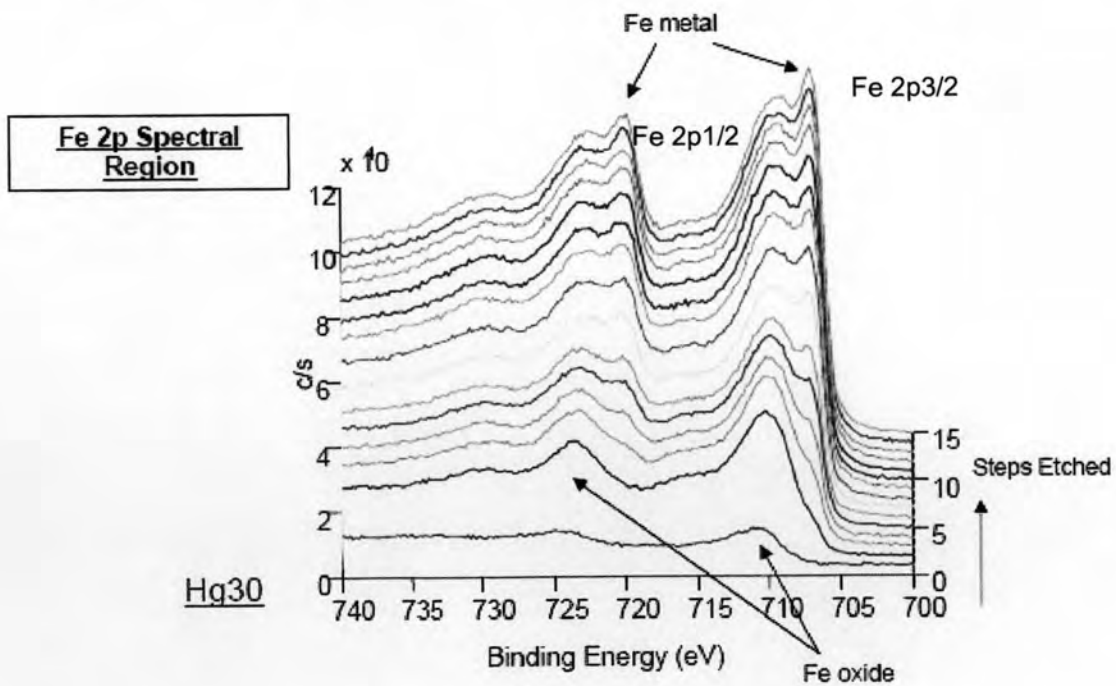
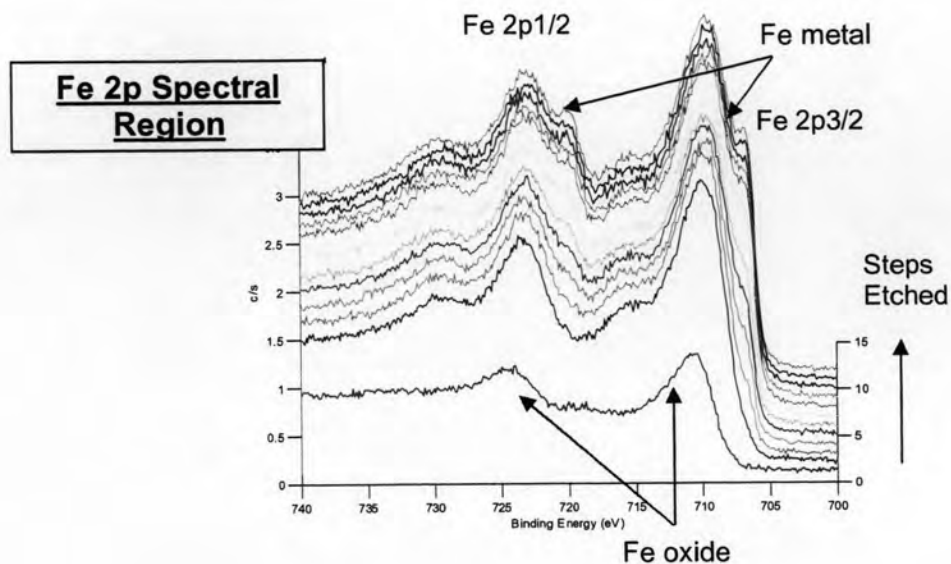


Figure 4-17 Depth Profile by XPS – Oxide Layers on the Surface of a 30 day Hg Adsorption Steel Coupon



### Hg60

**Figure 4-18** Depth profile by XPS – Oxide layers on the surface of a 60 day Hg adsorption steel coupon

Figure 4-16 to 4-18 show the XPS spectra of Fe<sub>2p3/2</sub> with the binding energy of 707 and 711 eV that match to those of Fe<sub>2p3/2</sub> of Fe and Fe<sub>2O3</sub>, respectively (Moulder, 1992). Also XPS spectra of Fe<sub>2p1/2</sub> shows the binding energies of 720 and 724 eV which also match to the binding energies of Fe<sub>1p1/2</sub> of Fe and Fe<sub>2O3</sub> respectively.

In the blank sample, Fe<sub>2O3</sub> is mostly present on the steel surface whereas Fe (metal) gradually increases and becomes more predominant through the course of the depth profile. However, for 30 and 90 day Hg treatment, much thicker layers Fe<sub>2O3</sub> were observed on the surface which also develops further into the depth profile in comparison to those of the blank coupon. This shows potential growing of Fe<sub>2O3</sub> layers on the surface of the steel coupon that may be contributed by effects of elemental Hg.

Withstanding these, the relationship of % Fe-oxide(out of the total Fe-metal at 349 nm depth) versus Hg adsorption periods were plotted the results of which are presented in Figure 4-19 below:

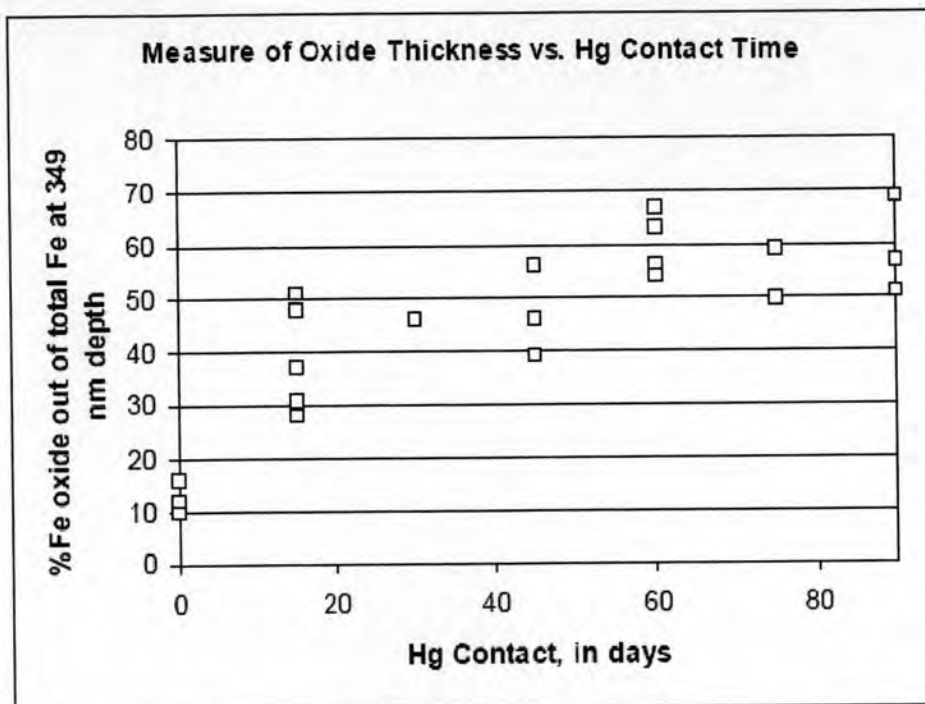


**Figure 4-19** Measurement of oxide thickness on the surface of Hg adsorption coupon surface with different Hg treatment periods.

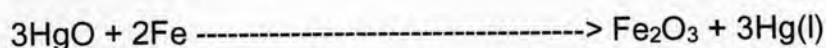
Figure 4-19 above shows that the longer the Hg contact time, the thicker the oxide layer is observed. It is therefore indicative that Hg may cause ferrous steel corrosion.

Two possibilities for the observation of the elemental Hg in the depth profile can be occurred including:

- a) Deposition of elemental Hg through the mechanisms 1) penetration of Hg into surface deposit such as rust layers, scales or salt precipitates. 2) Mercury deposit at previously damaged sites of the steel component 3) mercury in pore in the steel, which communicate with the

surface by way of channels 4) Hg in grain boundary zone such a result of transcrystalline diffusion (Zeittlitzer, 1997); and

b) By the reaction below:



The feasibility of the reaction is ascertained using Gibb' s formation energy and results of reviewing of the relevant literature are detailed below:

**Table 4-4** Gibb' s formation energy of the Hg(II) reduction by Fe(II)

3HgO + 2Fe = 3Hg + Fe2O3					
T (C)	deltaH (kcal)	deltaS (kcal)	deltaG (kcal)	K	Log (K)
0.000	-131.572	11.879	-134.816	7.528E+107	107.877
10.000	-131.560	11.922	-134.935	1.441E+104	104.159
20.000	-131.546	11.968	-135.055	4.950E+100	100.695
30.000	-131.531	12.018	-135.175	2.881E+097	97.695
40.000	-131.515	12.071	-135.295	2.700E+094	94.431
50.000	-131.498	12.124	-135.416	3.899E+091	91.591
60.000	-131.481	12.177	-135.538	8.345E+088	88.921
70.000	-131.463	12.229	-135.660	2.557E+086	86.408
80.000	-131.446	12.280	-135.782	1.089E+084	84.037
90.000	-131.428	12.329	-135.905	6.264E+081	81.797
100.000	-131.410	12.377	-136.029	4.755E+079	79.677

It was also reported that reduction of heavy metal (Hg), a toxic oxyanion (arsenate ion) and a chlorinated solvent (TCE) thus appear to be driven by the high reactivity of adsorbed Fe(II). Kinetic measurements at the nanomolar level of elemental Hg formed upon reduction of Hg(II) by Fe(II) in presence on the phlogopite particles provide further convincing evidence for reduction of Hg(II) coupled to oxidation of Fe(II) adsorbed. And indicate that

sorption of Fe(II) to mineral surfaces enhances the reduction rate of Hg(II) species (Charlet, 2002).

#### 4.2.2.3 Hg Depth Profiling of Hg Adsorption Coupon

The XPS depth profile analysis of Hg was undertaken with Hg adsorption steel coupons of 15, 30, 45, 60, 75 and 90 days, respectively. The results of Hg depth profile of these Hg treatments are presented in Figure 4-20 below:

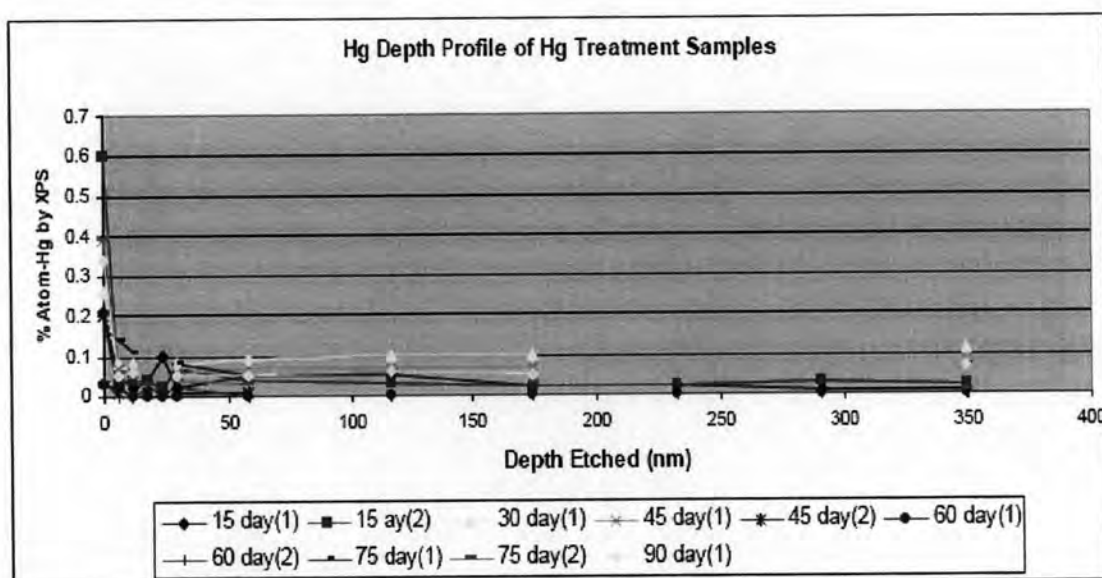


**Figure 4-20** Hg depth profile of the Hg adsorption steel coupons

It is noted here that for 30 and 90 day Hg treatments, the results of Hg depth profile of their duplicates were not analyzed. Figure 4-20 shows that Hg is more consolidated on the top surface to the depth of about 10 - 20 nm before it becomes persistent through the course of the depth profile with the Hg concentrations well below 0.1 % atom by XPS in all Hg treatments.

A study conducted on analysis of Hg impacted equipment, pipeline and tubing collected from a natural gas field known to have naturally occurring Hg reported that Hg is only adsorbed on the surface and did not penetrate into the steel structure. The results of the study were ascertained by

layered dissolution or milling steel samples for Hg analysis results (Zettlitzer, 1997).

The average Hg concentrations in % atom-Hg by XPS in the depth profile are presented in Figure 4-21 below:

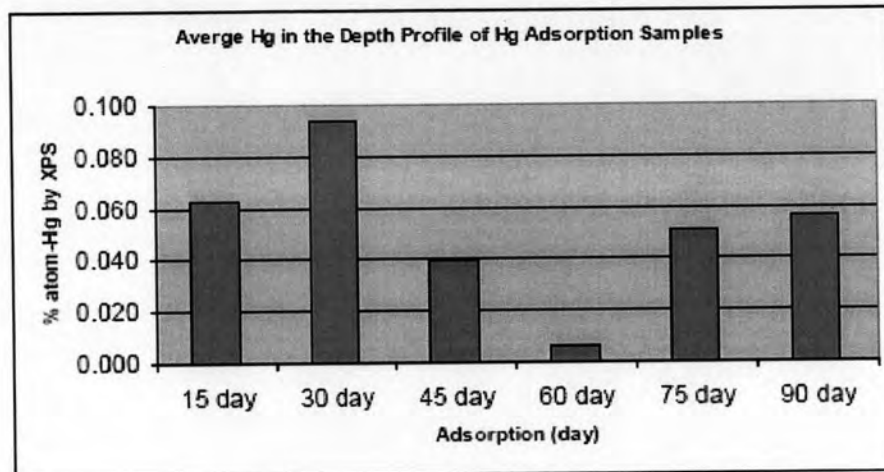


Figure 4-21 Average % Atom-Hg by XPS in the Depth Profile

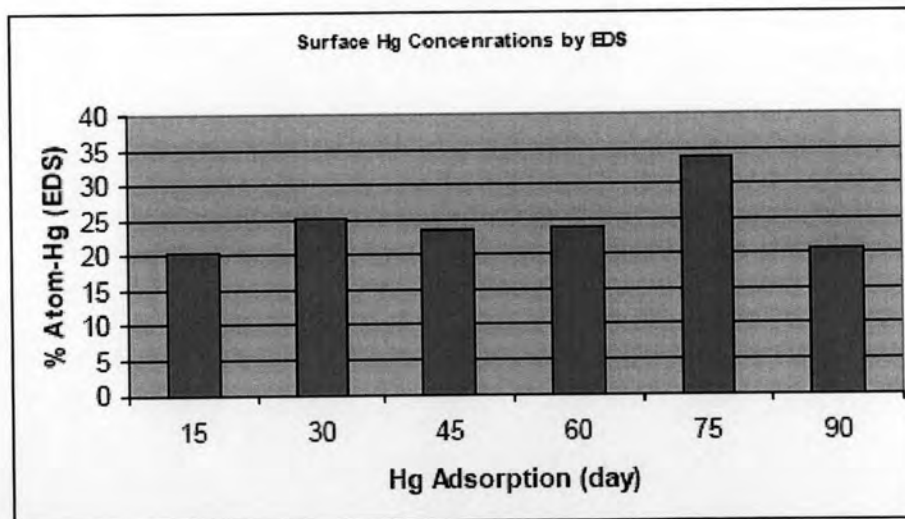


Figure 4-22 Average % Atom-Hg by EDS on the Hg adsorption Samples

Figure 4-21 shows that the average Hg level of % atom-Hg by XPS is very low relatively compared to initial surface Hg levels of % atom-Hg by the EDS. The lowest average % atom-Hg was observed at 60<sup>th</sup> day of Hg treatment with surface Hg of below 0.02 % atom-Hg by XPS whereas the highest was 0.9 % atom Hg by XPS found at 30<sup>th</sup> day of Hg treatment. Both Figures show that there is no reasonable correlation existed between the initial Hg concentrations adsorbed on the surface and those found in the depth profile.

### **4.3 Hg Decontamination**

Hg decontamination experiments were conducted to identify the effects of Hg adsorption times and iodine concentrations. In all Hg decontamination experiment, excessive Potassium Iodide (KI) of 2.0 M was designated to all experimental treatments to ensure that all mercuric generated would be adequately stabilized. The Hg decontaminated steel coupons were submitted for surface analysis including SEM-EDS, XRD and XPS, respectively, in the same sequences as those of Hg adsorption samples. The results of the analysis are discussed as the following:

#### **4.3.1 Surface Morphology after Decontamination**

The surface morphology of the decontaminated samples was characterized by SEM of which their illustrations are presented as the following:

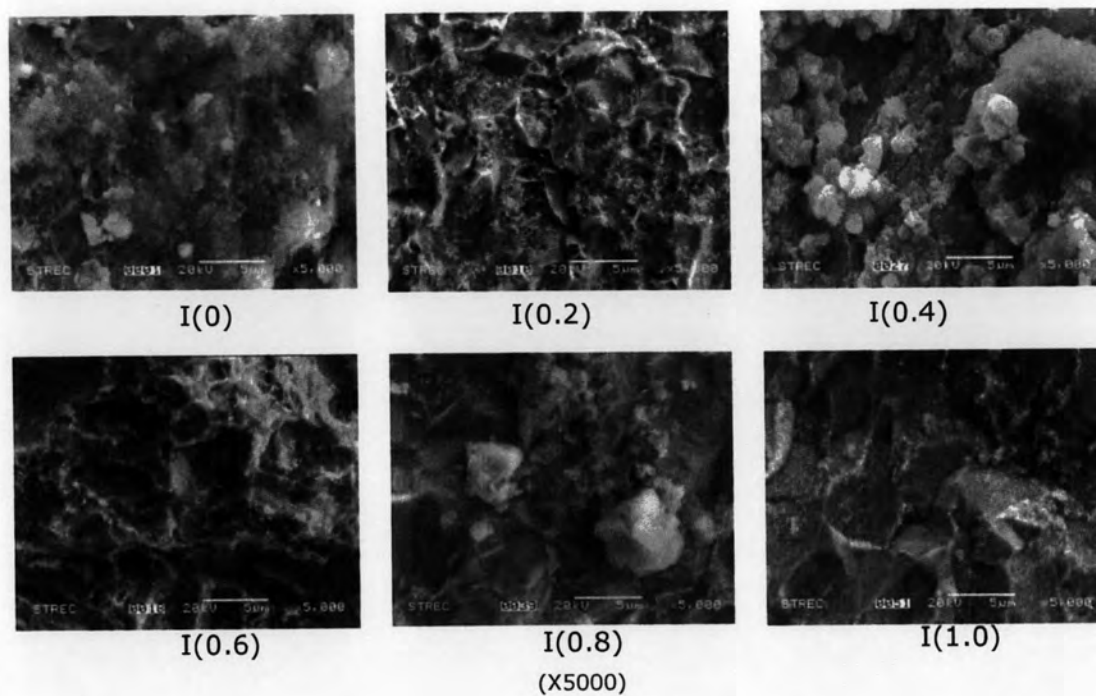


**Figure 4-23** SEM illustrations of blank after decontamination by varied  $I_2/2.0$  Molar KI

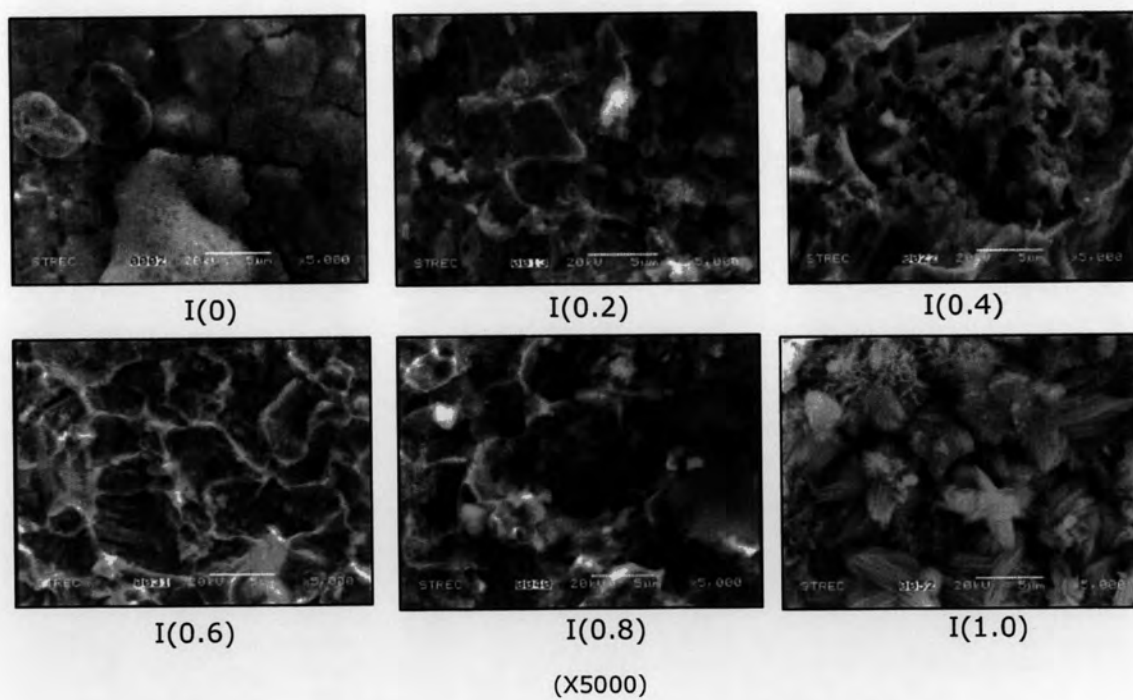


**Figure 4-24** SEM illustrations of Hg 15 day adsorption samples after decontamination by varied  $I_2/2.0$  Molar KI



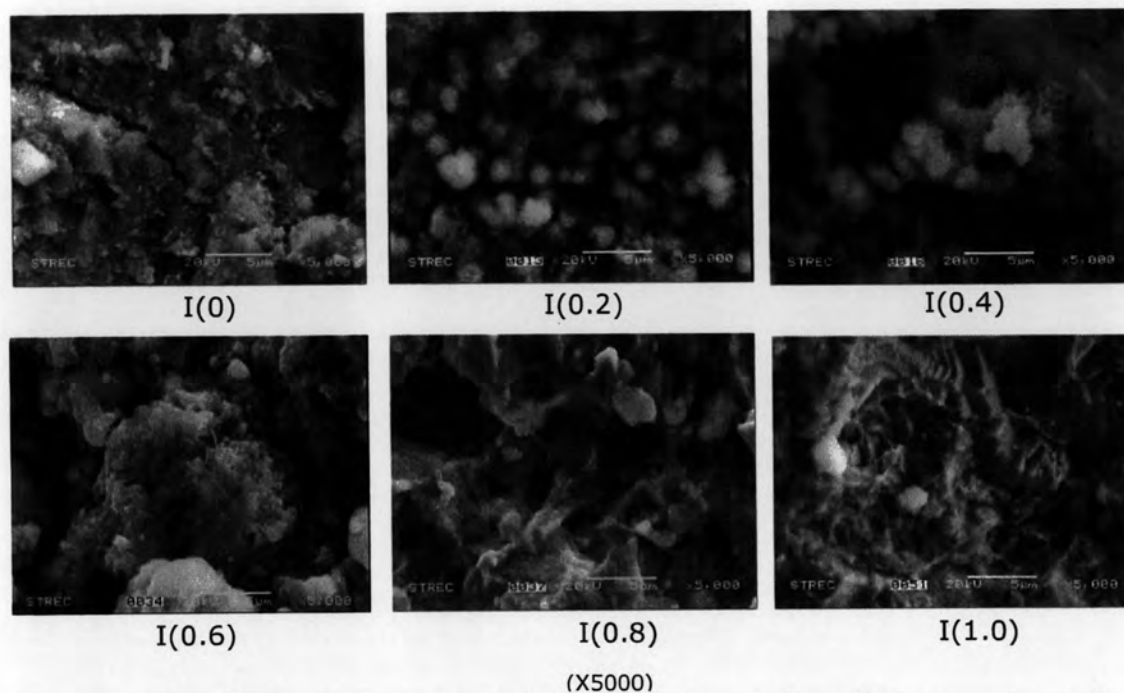


**Figure 4-25** SEM illustrations of Hg 30 day adsorption samples after decontamination by varied  $I_2/2.0$  Molar KI

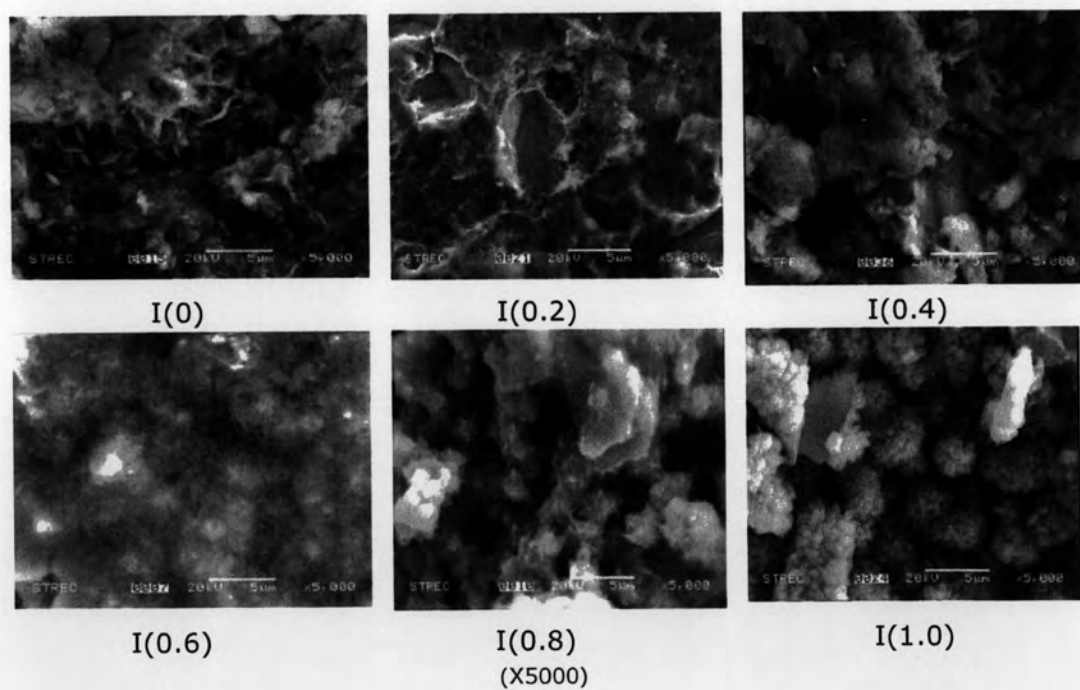


**Figure 4-26** SEM illustrations of Hg 45 day adsorption samples after decontamination by varied  $I_2/2.0$  Molar KI

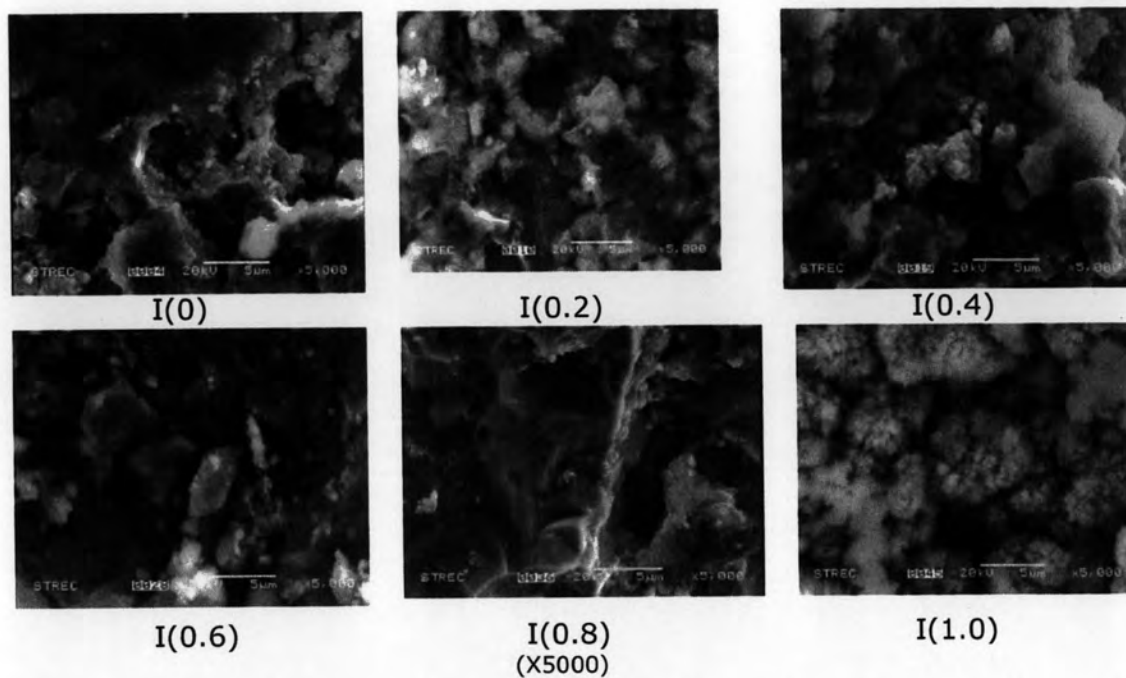


**Figure 4-27** SEM illustrations of Hg 60 day adsorption samples after decontamination by varied  $I_2/2.0$  Molar KI

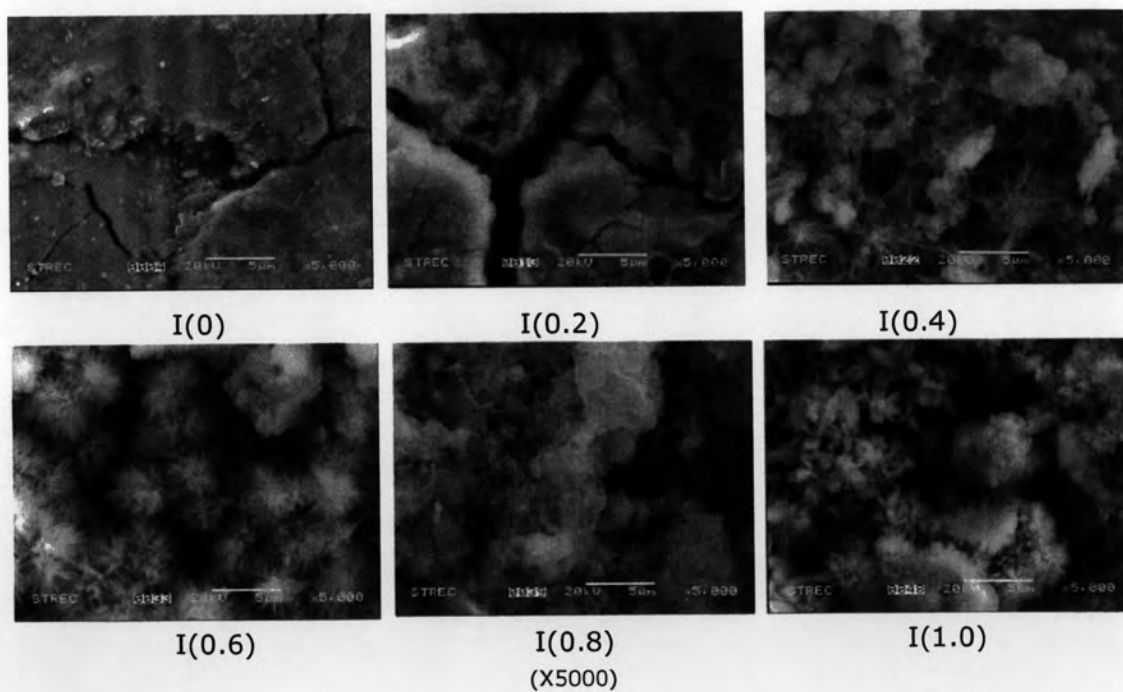


**Figure 4-28** SEM illustrations of Hg 75 day adsorption samples after decontamination by varied  $I_2/2.0$  Molar KI

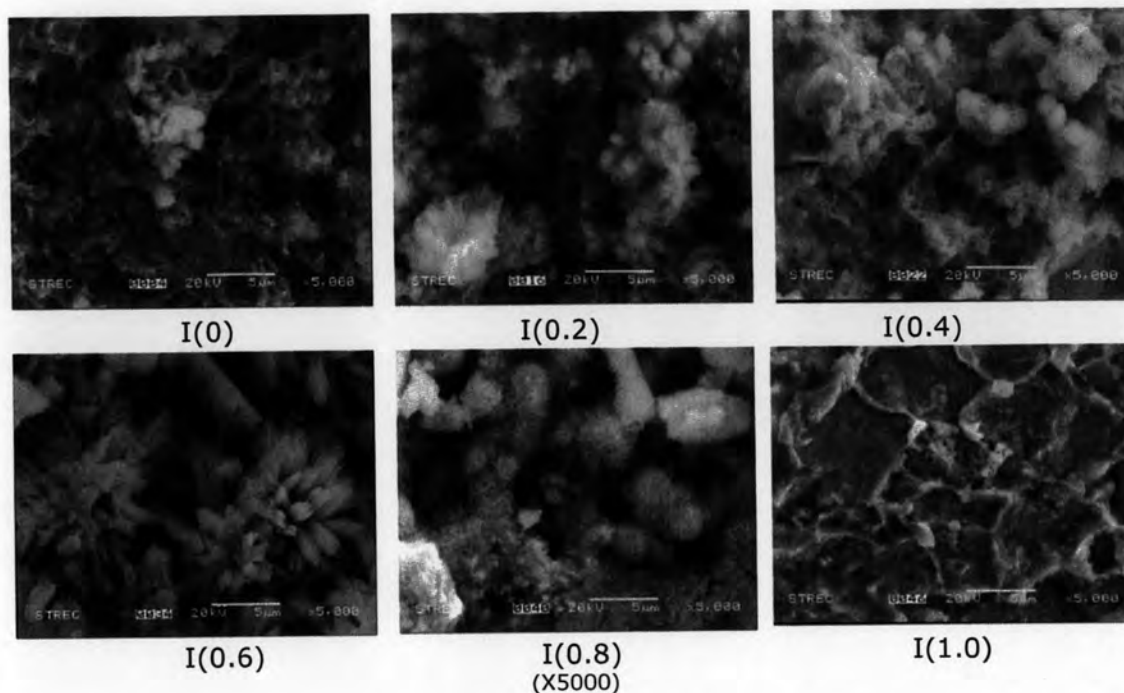


**Figure 4-29** SEM illustrations of Hg 90 day adsorption samples after decontamination by varied  $I_2/2.0$  Molar KI

Based on the above Figures, the following are discussed:

- After decontamination, no Hg droplets were observed on the surface of all decontaminated samples. However, this observation has to be ascertained using other surface instrumentation analysis to be discussed in the following sections; and
- The higher iodine concentration, the more surface corrosion was observed. They also indicated that Hg in the depth profile may have been removed from the depth profile due to corrosion effect of the lixiviant employed.

### 4.3.2 Surface Chemistry after Decontamination

#### 4.3.2.1 EDS Analysis – After Decontamination

The EDS analysis is undertaken to characterize surface chemistry of the Hg decontaminated coupons the results of which are presented in Appendix C and the examples of their profiles are shown as the following:

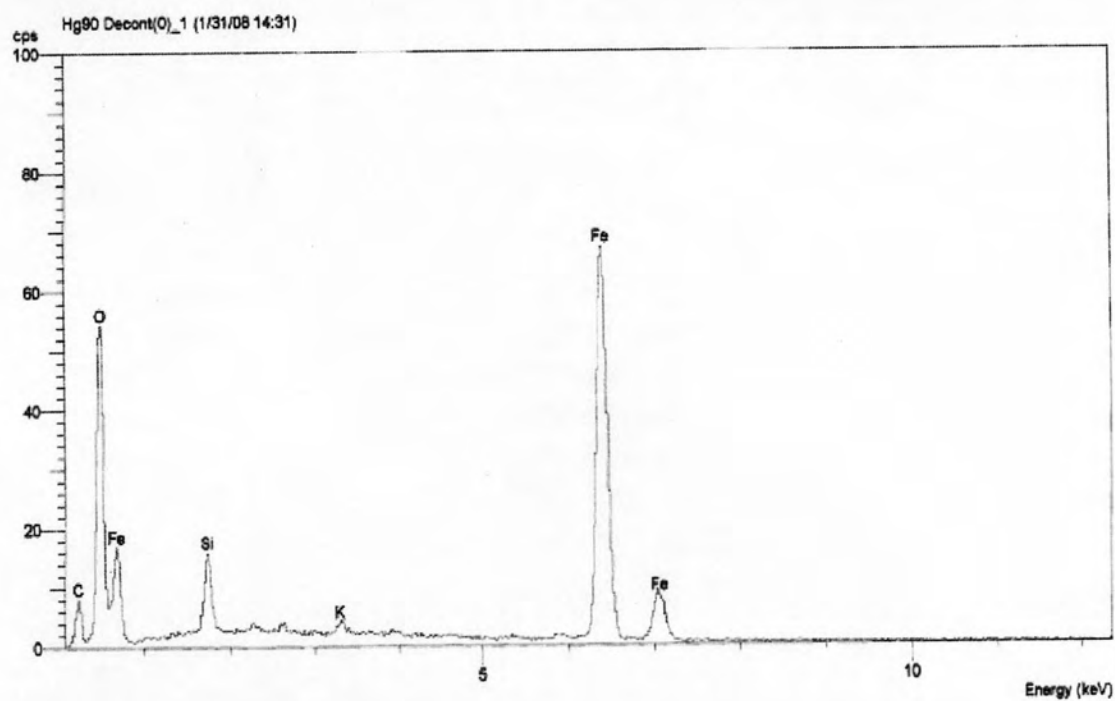


**Figure 4-30** EDS profile of a 90 day Hg adsorption sample decontaminated with 2.0 Molar KI

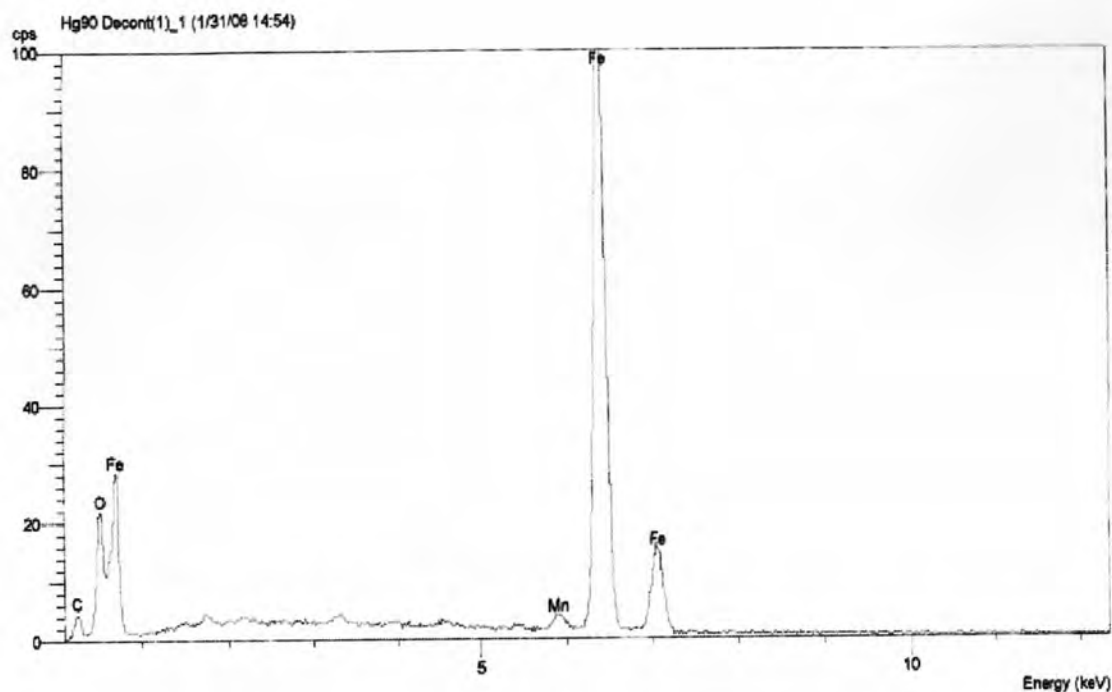


**Figure 4-31** EDS profile of a 90 day Hg adsorption sample decontaminated with 0.2 Molar  $I_2$ /2.0 Molar KI

The EDS analysis results of all Hg decontaminated samples show that there was no Hg detected on the surface. It is noted here that the detection limit of Hg using the EDS technique is less than 1% atom of Hg. These also include all treatment without  $I_2$  (only 0.2 M of KI was present) as shown in Figure 4-30. However, the results of the EDS analysis alone could not be used for sole conclusion at this stage due to its limited detection limit. To ascertain this, the results of more surface sensitive analysis including XPS were further to be used and discussed in the following sections;

#### 4.3.2.2 XRD Analysis – After Decontamination

The XRD analysis was undertaken no later than a week after the decontamination steel coupons had been submitted for the analysis. The XRD profiles of all Hg decontaminated treatment are presented in Appendix D, of which the summarized XRD profile for each I<sub>2</sub> treatment of all Hg adsorption periods are presented in Figures below:

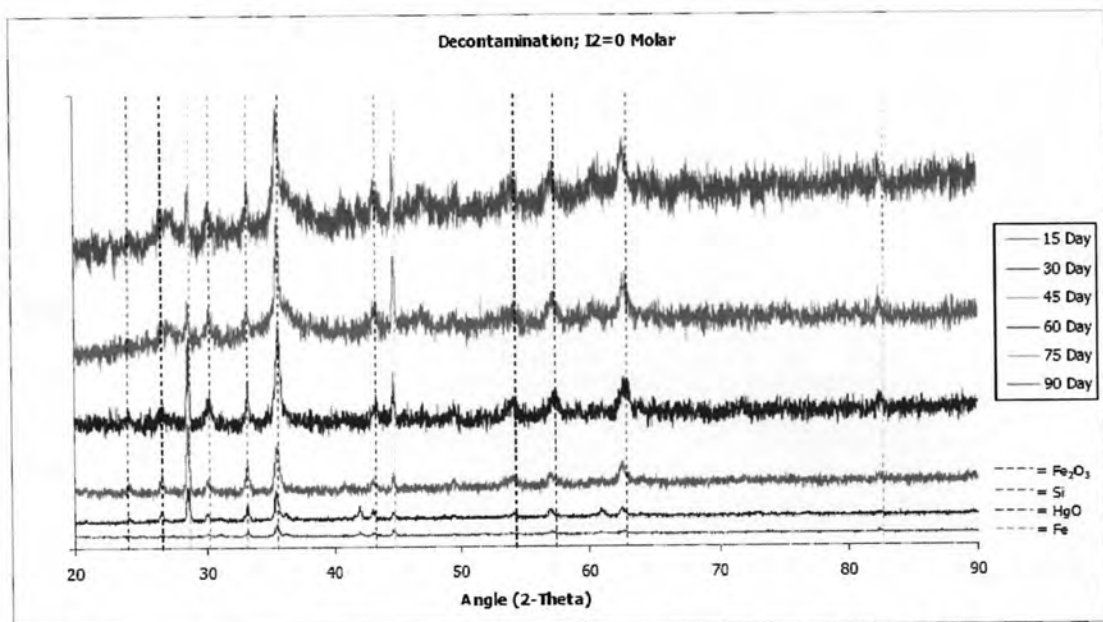


**Figure 4-32** The XRD profiles of decontaminated samples of without iodine + 2.0 Molar KI

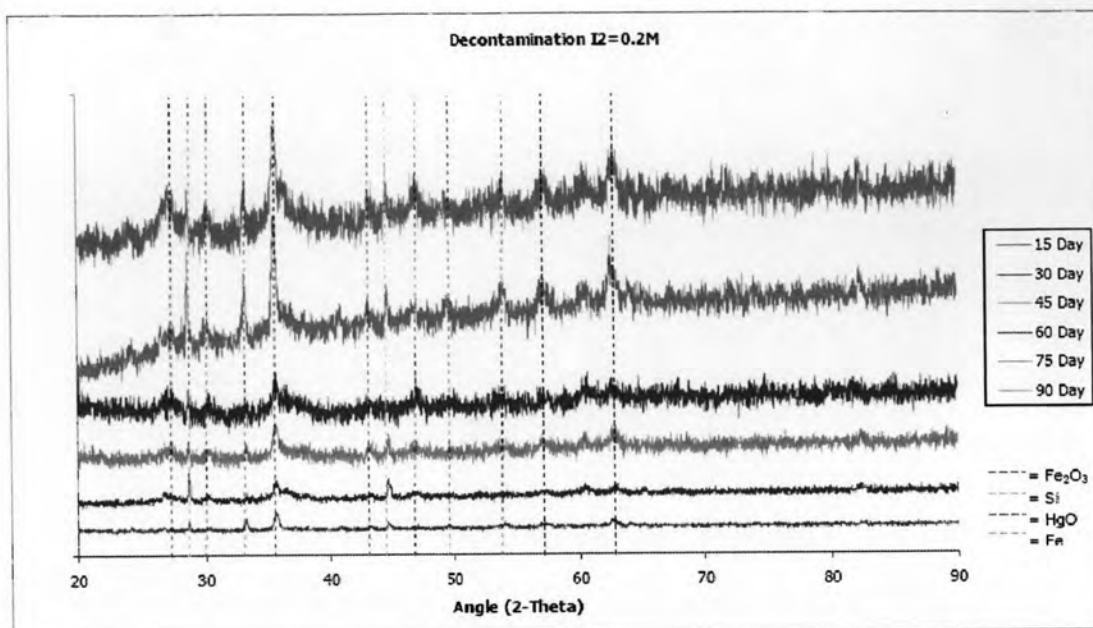


**Figure 4-33** The XRD profiles of decontaminated samples with 0.2 M I<sub>2</sub> + 2.0 M KI

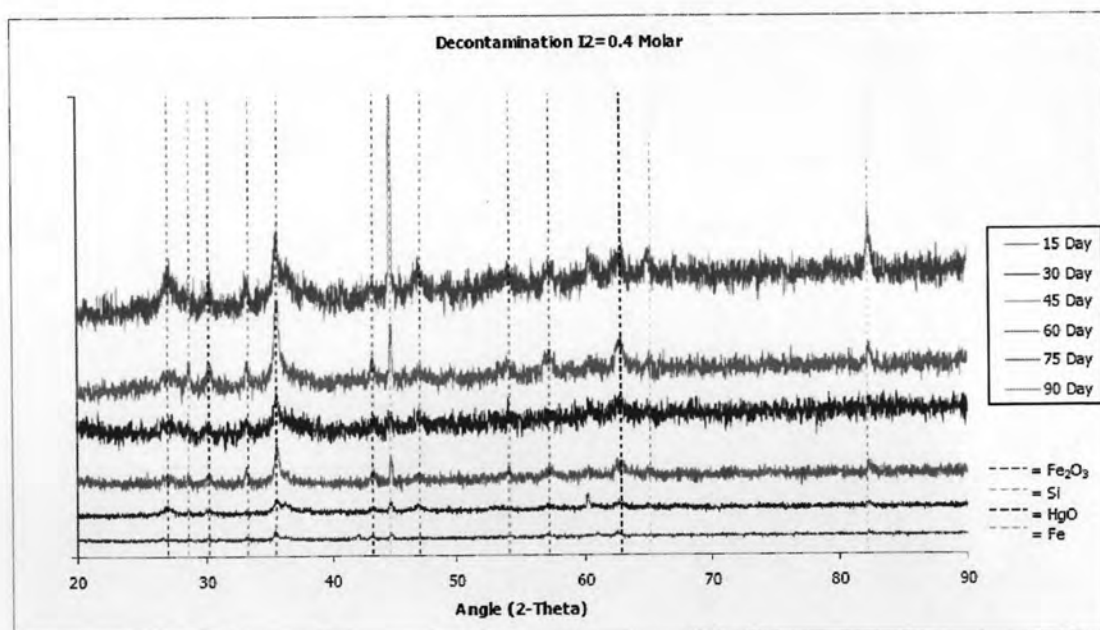


**Figure 4-34** The XRD profiles of decontaminated samples with 0.4 M I<sub>2</sub> + 2.0 Molar KI

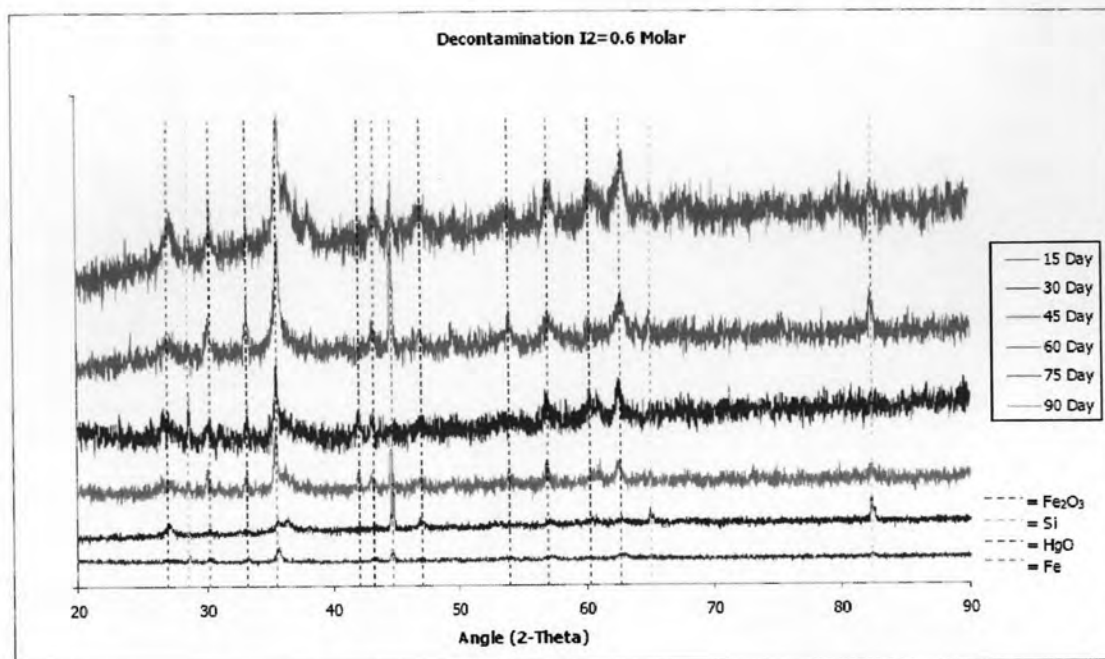


Figure 4-35 The XRD profiles of decontaminated samples with 0.6 M I<sub>2</sub> + 2.0 Molar KI

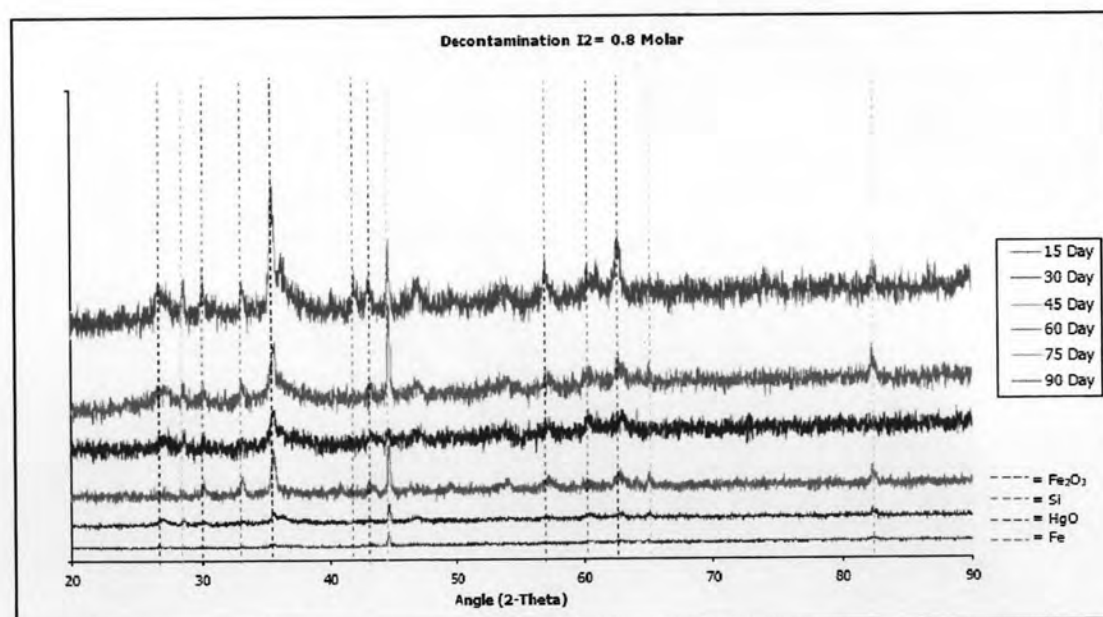
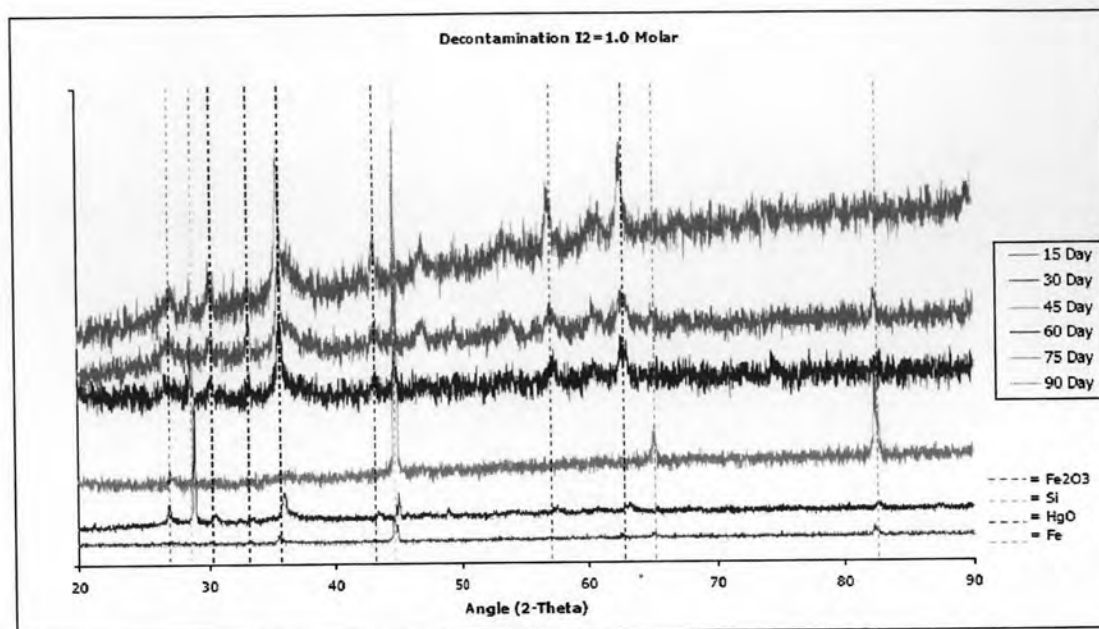


Figure 4-36 The XRD profiles of decontaminated samples with 0.8 M I<sub>2</sub> + 2.0 Molar KI





**Figure 4-37** The XRD profiles of decontaminated samples with 1.0 M I<sub>2</sub> + 2.0 Molar KI

The results of XRD analysis show presence of HgO on the surface the overall results of which can be summarized in Table 4-4 below:

**Table 4-5** Presence of HgO on the Surface of Decontaminated Steel Coupons with Different Adsorption Periods – XRD analysis

Hg Adsorption(day)	Iodine Concentration (X) Molar/2.0 Molar KI					
	0	0.2	0.4	0.6	0.8	1
15	√	√	√	√	X	X
30	√	√	√	X	X	X
45	√	√	√	√	√	X
60	√	√	√	√	√	√
75	√	√	√	√	√	√
90	√	√	√	√	X	X

Note: √ detected and X not detected

Table 4-5 suggests that HgO is present on the surface of almost all decontaminated steel coupon samples, except those of 15, 30 and 90 day

Hg treatment respectively, at high I<sub>2</sub> concentration e.g. >0.6 M. Based on their initial surface concentrations of Hg (reported by EDS analysis), it was found that initial surface Hg concentrations of 15, 30 and 90 day Hg treatment were relatively low and in the presence excessive I<sub>2</sub> levels, HgO formed on their surfaces may have been totally dissolved and removed by iodine.

#### 4.3.2.3 XPS Surface Analysis

The XPS surface analysis was performed on the decontaminated samples to characterize surface chemistry and also Hg concentrations that may present on the steel coupon surface after decontamination.

In order to obtain more representative results, the XPS surface analysis was conducted with the selected Hg and Iodine treatments. For Hg treatment, they were classified using initial surface Hg concentrations as discussed earlier in Section 4.2.2.1 including:

- Group 1: low – 15 and 90 day Hg treatments (but 90 day Hg treatment was selected for the experiment);
- Group 2: moderate – 30, 45 and 60 day Hg treatments (but 30 day Hg treatment were selected for the experiment); and
- Group 3: high - 75 day Hg treatment were selected.

Also certain concentrations of I<sub>2</sub> were also selected including no iodine, 0.2, 0.6 and 1.0 M, respectively, ensuring that it covers the whole concentration ranges. These lixiviant solutions all contain the same concentrations of KI at 2.0 M. Based on the above, the results of XPS analysis are presented as the following:

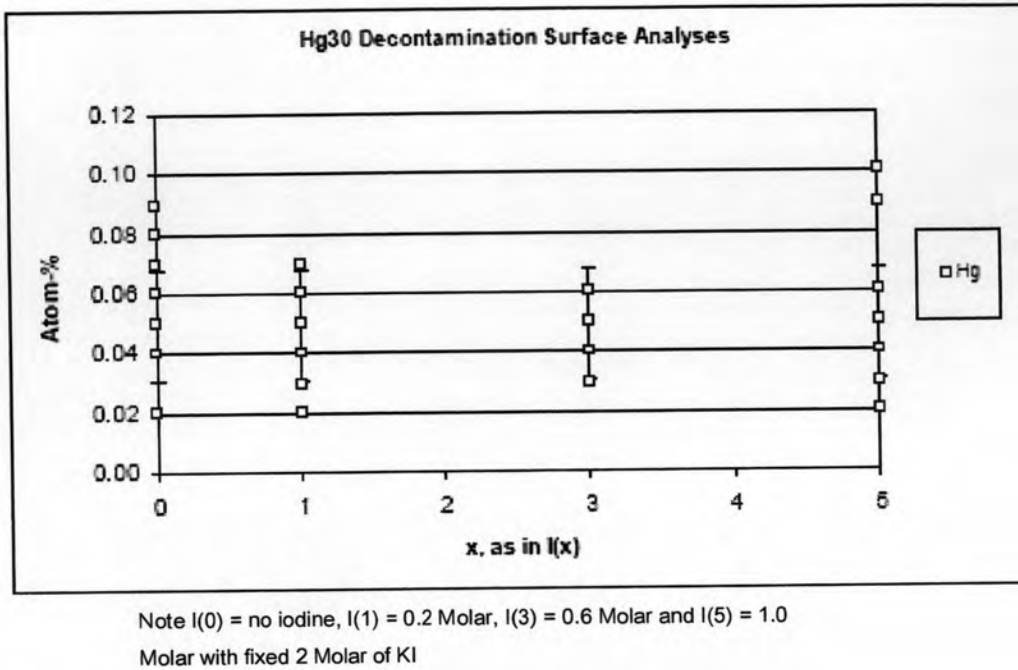


**Figure 4-38** XPS surface analysis of decontaminated samples of 30 day Hg adsorption

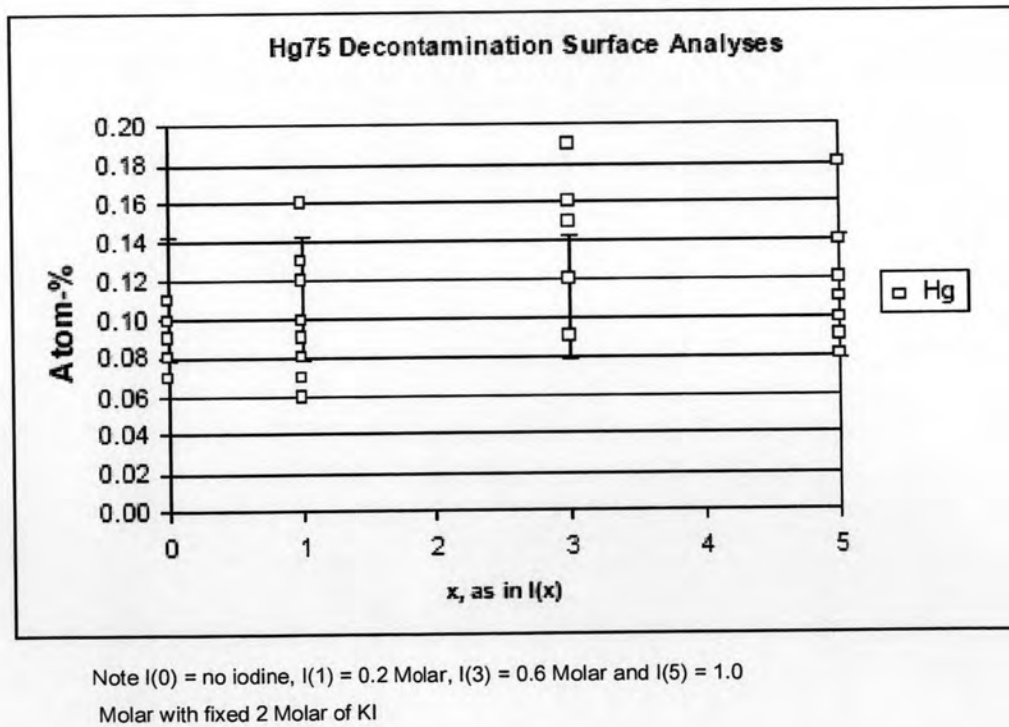
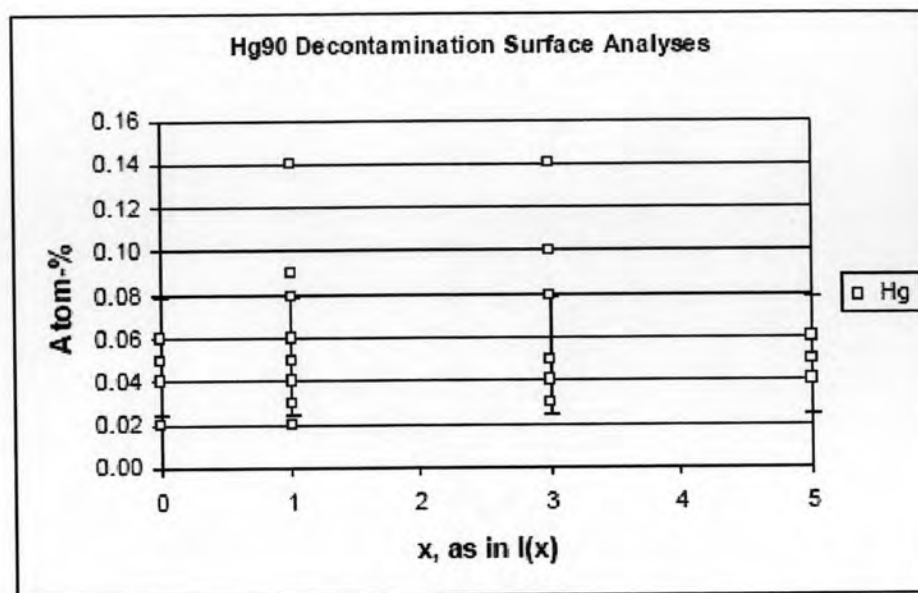


**Figure 4-39** XPS Surface analysis of decontaminated samples of 60 day Hg adsorption



Note I(0) = no iodine, I(1) = 0.2 Molar, I(3) = 0.6 Molar and I(5) = 1.0 Molar with fixed 2 Molar of KI

**Figure 4-40** XPS surface analysis of decontaminated samples of 60 day Hg adsorption

Figures above are discussed as the following:

- Even though residual surface Hg could not be detected using the EDS technique, but the XPS technique, due to higher detection limit;
- After decontamination, surface Hg concentrations are still varied from one to other locations on the steel coupon surface which may be attributed by surface heterogeneity;
- The statistical analysis of the XPS results of surface Hg concentrations after decontamination using Single-factor ANOVA technique revealed that in 30 day Hg treatment, average surface Hg concentrations are not significantly different in all I<sub>2</sub> treatment ( $F_{\text{critical}} = 2.8 > F_{(0.05,3,12)} = 1.34$ ).

- The same statistical analysis applied to 75 day treatment revealed that the surface Hg concentrations are significantly different in each I<sub>2</sub> treatment ( $F_{\text{critical}} = 2.8 < F(0.05, 3.38) = 5.3$ ).
- The same statistical analysis applied to 90 day treatment revealed that the surface Hg concentrations are not significantly different in each I<sub>2</sub> treatment ( $F_{\text{critical}} = 2.8 > F(0.05, 3.36) = 1.07$ ).

The average surface Hg concentration after decontamination at each I<sub>2</sub> treatment is presented in Figure 4-42 below:

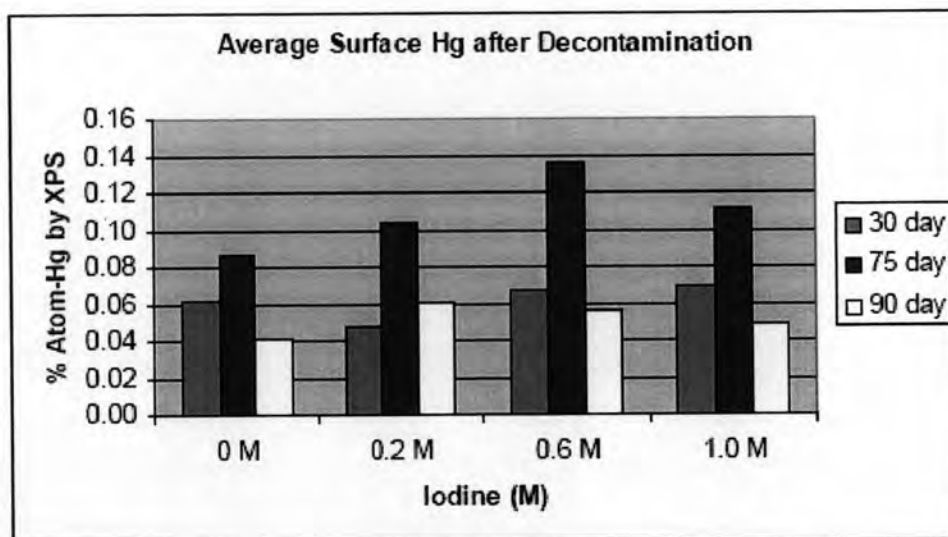


**Figure 4-41** Residual surface Hg concentrations with varied I<sub>2</sub>

Figure 4-41 shows that at I<sub>2</sub> treatment of 0 and 0.2 M there were no major differences in residual surface Hg concentrations in all Hg treatment periods. Their surface Hg concentrations were all reduced to approximately less than 0.1%. However, it is hard to conclude at this stage that the treatment without iodine is recommended to effectively decontaminate Hg on the surface, because washed-off Hg droplet still requires I<sub>2</sub> to stabilize it and effectiveness in Hg removal in the depth profile has yet to be determined.

#### 4.3.4 Hg Depth Profile after Decontamination

The XPS depth profile analysis were undertaken with 30, 75 and 90 day Hg treatments in combination with  $I_2$  treatments of 0, 0.2, 0.6 and 1.0 M, respectively. The experiments were designed to ensure the representativeness of the results could still be obtained within the provided resource and time limits. The results of the Hg depth profile analysis and discussion are presented as the following:

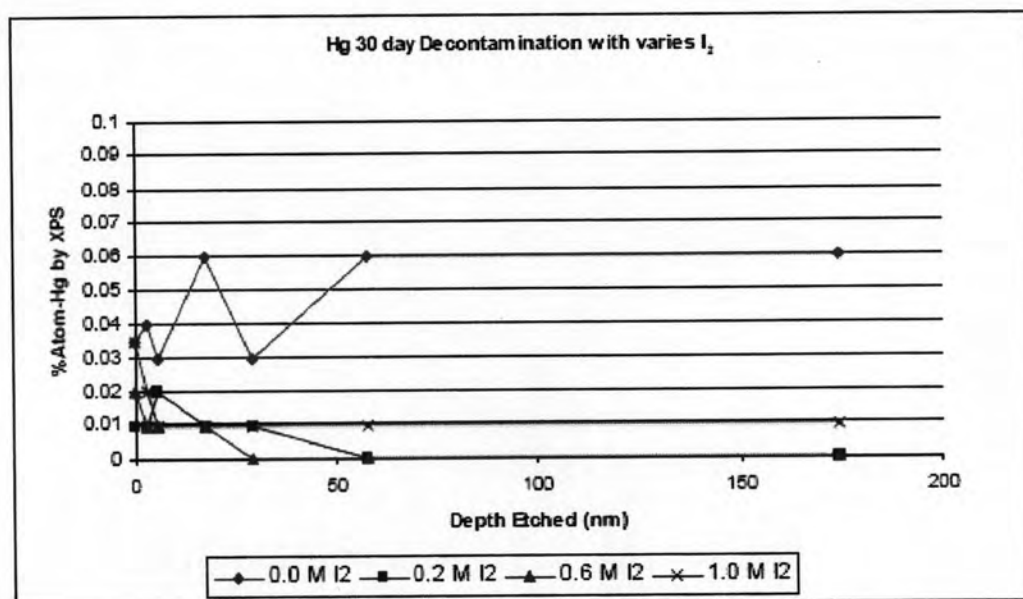


**Figure 4-42** Hg depth profile of 30 day Hg Adsorption with varied  $I_2$  concentration and fixed 2.0 M KI

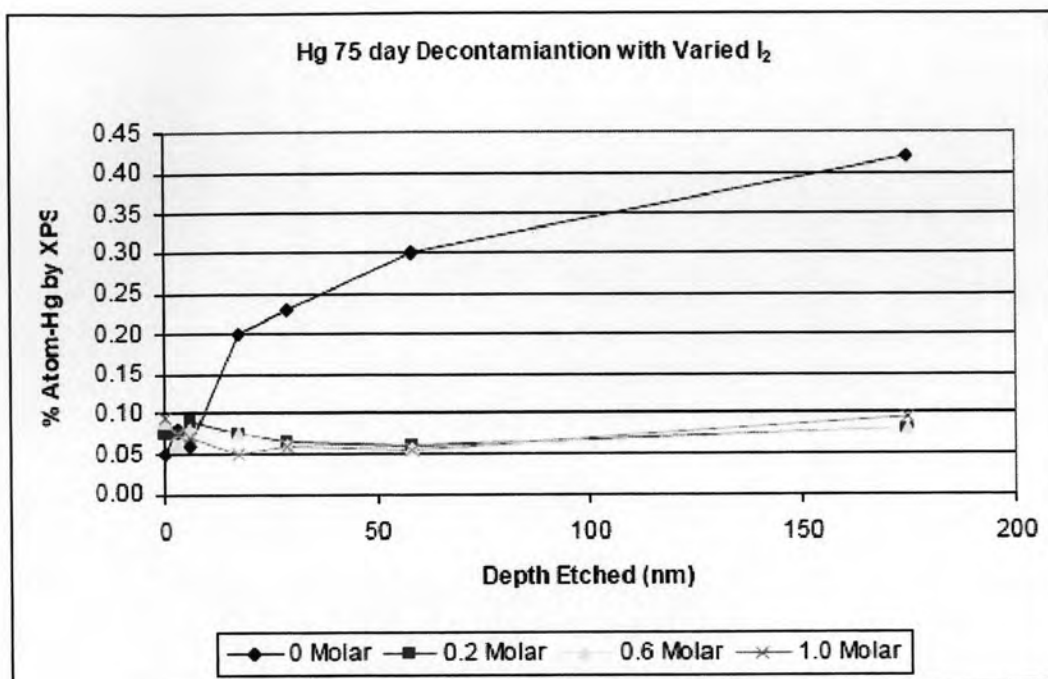


**Figure 4-43** Hg depth profile of 75 day Hg adsorption with varied I<sub>2</sub> concentration and fixed 2.0 M KI

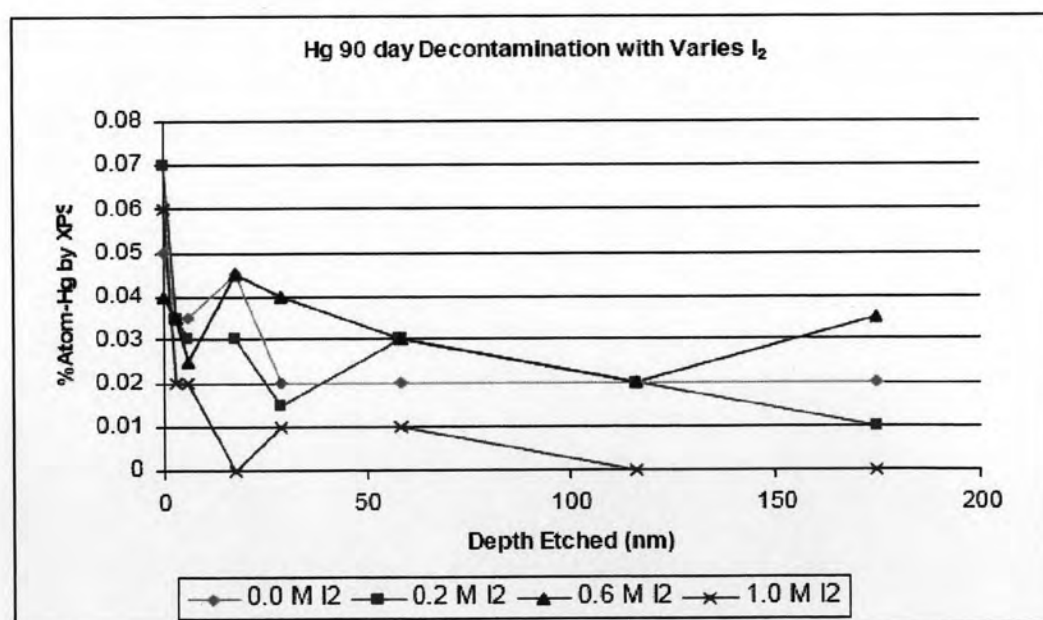


**Figure 4-44** Hg depth profile of 90 day Hg adsorption with varied I<sub>2</sub> concentration and fixed 2.0 M KI

Figure 4-42 to 4-44 above suggest the following:

- At 90 day Hg treatment (low initial Hg levels), Hg decreased rapidly from the surface to the depth of about 50 nm in all I<sub>2</sub> treatment with % atom of Hg by XPS well below 0.05 prior to be persistent through out the course of the depth profile;
- However, for higher Hg levels including 30 and 75 day Hg treatments, Hg decreases rapidly from the top surface to the depth about 50 nm and stays persistent through the course of the depth profile in all I<sub>2</sub> treatment, except those of without I<sub>2</sub>. Their Hg in the depth profile show different response that increased instead of decreased;
- The results above suggest that without I<sub>2</sub> in the decontamination solution, Hg in the depth profile especially with high initial surface Hg level; may not be reduced. This may be due to the I<sub>2</sub> effect that cause corrosion of metal surface and also dissolved Hg that stay in the depth profile as discussed earlier in Section 4.3.1; and
- Based on the above results, it is suggested that I<sub>2</sub> at 0.2 M could effectively removed Hg in the depth profile at the surface Hg concentrations used in the experiments.

#### **4.4 Surface Mercury Measurement by Handheld XRF Analysis**

Sampling and analysis of Hg impacted steel samples poses both logistic and technical implications. Collection, including cold cutting and also shipment of the samples for laboratory analysis, can cause losses of elemental Hg through volatilization. These processes sometime take a few days to weeks. The results of our study indicate that the majority of Hg (elemental) could be lost significantly through volatilization. Therefore in-situ Hg measurement technique is more preferred alternative for the industry.



The currently developed technology of in-situ Hg measurement was reviewed and it was found that current models of handheld X-ray Fluorescent Spectrometer (XRF), available commercially, can also be used for in-situ analysis of surface on steel surface. The results of the reviews and the data obtained are presented as the following;

A handheld XRF instrument was obtained from a manufacturer to measure surface Hg on the same coupon samples used in the XPS analysis of which surface Hg levels ranged 0 to 1.15 % atom-Hg. The XPS analysis area is 100 microns by 1.4 mm, whereas the handheld XRF instrument was 1 cm diameter. The results of the above correlations are presented in Figure 4-46 below:

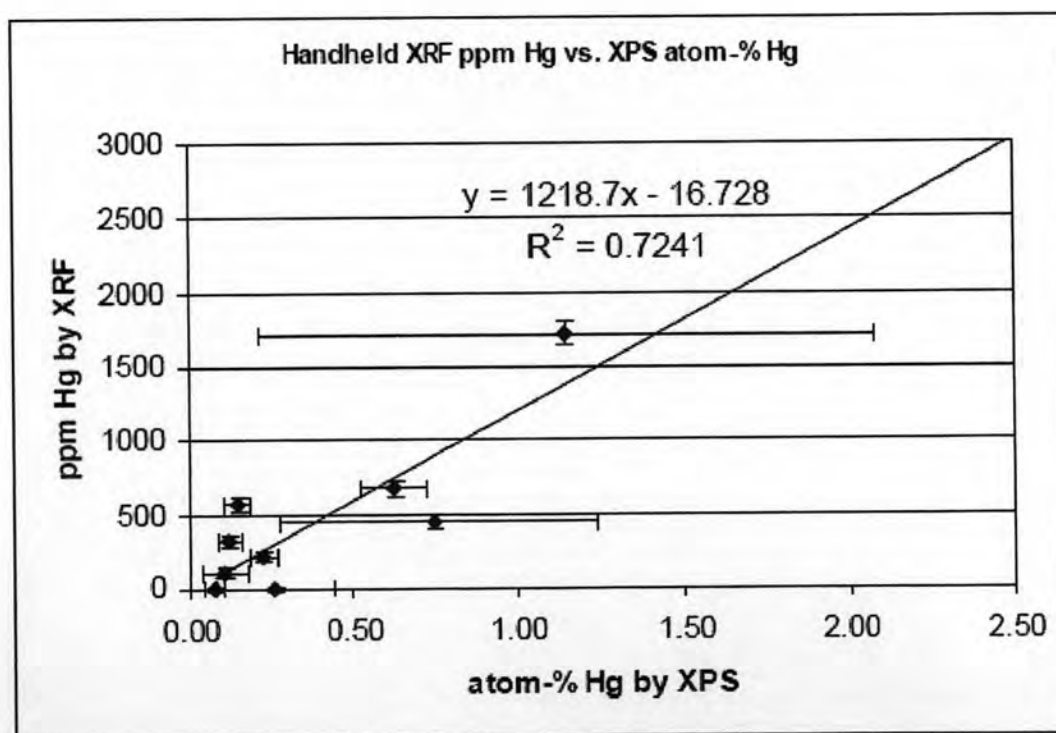


**Figure 4-45** Correlations of % atom-Hg between handheld XRD and the XPS surface Hg analysis

Based on Figure 4-45, it shows that there is a reasonable correlation between the handheld XRF and the XPS on the surface Hg levels ( $R^2 = 0.724$ ). Based on the correlation, 1 % atom of Hg by XPS correspond to 1,200 ppm (or kg/mg) of Hg by the handheld XRF (HXRF). It is noted here that the correlations, at lower surface Hg concentrations (< 0.5 % atom-Hg by XPS); deems to have better coefficient and that the HXRF reading at lower concentrations give more reliable reading.

It is noted that these measured concentrations are those present on the top most surface of the steel coupons. The handheld XRF measures up to 2  $\mu\text{m}$  in depth which is much less than 1% (by weight) of the whole steel coupon. As the results, Hg concentrations by total weight of material analyzed could be more than 100 time less. It also suggests that the handheld XRF could potentially be used to analyze surface Hg on steel surface in-situ.